M 2020

U.PORTO
FEUP FACULDADE DE ENGENHARIA
UNIVERSIDADE DO PORTO

HIGH ENERGY EFFICIENT AND STABLE SOLAR REDOX FLOW BATTERY

TIAGO FILIPE ALBERTO ANTUNES

DISSERTAÇÃO DE MESTRADO APRESENTADA
À FACULDADE DE ENGENHARIA DA UNIVERSIDADE DO PORTO EM
MIEQ – MESTRADO INTEGRADO EM ENGENHARIA QUÍMICA

Master in Chemical Engineering

High energy efficient and stable solar redox flow battery

Master dissertation

of

Tiago Filipe Alberto Antunes

Developed within the course of dissertation

held in

LEPABE – Laboratory for Process Engineering, Environment, Biotechnology and Energy

Supervisor: **Dr. Paula Dias**

Co-supervisor: **Prof. Adélio Mendes**

July 2020

Acknowledgment

Firstly, I would like to show my gratitude towards my supervisor, Dr. Paula Dias. I have to thank her for all the help, support, guidance and knowledge that she gave me during the entire realization of this work. Even with all the “adversity” that she faced in the last few months, she always did her best to make sure that I did the best job that I could and to help me in any way she could.

I also have to thank Professor Adélio Mendes for giving me the opportunity to work in this subject and, most importantly, for making me get out of my “comfort zone” and evolve academically and professionally.

I am very thankful to all the members of the Solar Group for making me feel welcome in the workspace and for the help that they gave me. I have to thank, in particular, Filipe Moisés, Telmo Lopes and António Vilanova for all the assistance they provided and for everything that they taught me.

To all my friends I show my appreciation, they helped throughout this academic journey and are always there when I need them. To my girlfriend, Rita Borges, I am thankful for all the encouragement and unconditional support that she gave me during stressful and non-stressful times.

Lastly, I am grateful to my dad, Carlos, my sister, Inês and my aunt, Judite, for always been there for me and making everything that I achieved possible.

This work was financially supported by: i) Base Funding - UIDB/00511/2020 of the Laboratory for Process Engineering, Environment, Biotechnology and Energy – LEPABE - funded by national funds through the FCT/MCTES (PIDDAC); and ii) Projects SunStorage POCI-01-0145-FEDER-016387, funded by European Regional Development Fund (ERDF), through COMPETE2020 - Programa Operacional Competitividade e Internacionalização (POCI), by FCT, SunFlow POCI-01-0145-FEDER-030510 and HopeH2 POCI-01-0145-FEDER-030760, both funded by FEDER funds through COMPETE2020 - POCI and by national funds (PIDDAC) through FCT/MCTES.

Abstract

Planet Earth is facing extreme environmental problems caused by economic growth. The coronavirus pandemic changed politics, health concerns, economy and habits of the everyday life. This sudden "stop" of the entire World is, and will be, responsible for great changes, and it will, hopefully, turn even more attention towards the environment. Sustainable development path requires faster decarbonization of the energy by a collaborative effort of the population and the evolution of technologies used. Renewable energies will, undeniably, be part of the future, and this global crisis could be the turning point to even more changes in the way energy is produced and harnessed.

Towards a "greener" future, sunlight is probably the most convenient renewable energy source; however, given its intermittent nature, solar energy storage is required, and it must display a low environmental life cycle impact. Solar redox flow cells (SRFC) show great promise for the in-loco production of thermal and electrical energy for buildings. These devices combine the working principles of photoelectrochemical (PEC) and redox flow cells in a single system. The PEC cell provides the redox reactions with the energy needed for converting the sunlight into a storable liquid electrochemical fuel, mimicking photosynthesis. Electrolytes also convert sunlight-to-thermal energy, which can be used for thermal comfort and sanitary waters. The stored chemical energy can then be easily and efficiently converted into electricity at a redox flow battery (RFB), which is already the most competitive battery technology for stationary applications. This technology is at laboratory scale, and this work aims to make a path for future research and industrial implementation.

An economic analysis was conducted for SRFCs to understand their potential to be technically and economically viable. The viability of such devices is only possible if four requirements are simultaneously fulfilled: high performance, low cost, sustainability, and robustness. This work comprises the comparison of different device designs (standalone SRFC, SRFC coupled with PV panels and SRFC with solar concentrators), operating conditions and materials combinations between photoelectrodes (hematite and bismuth vanadate) and electrolytes (ferrocyanide/anthraquinone AQDS 2,7 and ferrocyanide/polyoxometalate SiW_{12}), locations (Portugal and Denmark) and scales (1 kW and 20 kW installations). The best scenario studied for SRFCs was based on the use of hematite as photoelectrode and ferrocyanide/AQDS redox pairs in the electrolyte, located in Denmark, and with a 20 kW installation. This scenario requires 2346 PEC cells to produce 293.4 GWh in 20 years (viable for neighborhood applications), has a LCOE of 0.17 €·kWh^{-1} and a payback time of 11.2 years, which are values close to an actual investment in PV panels and vanadium RFBs to produce the same power.

Keywords (theme): **Solar Energy, Electrochemical fuels, Solar Redox Flow Cells, Off-grid electrification, Economic Analysis**

Resumo

O planeta Terra está a enfrentar extremos problemas ambientais causados pele crescimento económico. A pandemia do coronavírus mudou a política, cuidados de saúde, a economia e os hábitos do dia a dia. Esta súbita "paragem" de todo o Mundo é, e será, responsável por grandes mudanças, e dará ainda mais atenção ao ambiente. O desenvolvimento de um caminho sustentável requer uma descarbonização rápida da energia através de um esforço coletivo da população e da evolução das tecnologias utilizadas. Energias renováveis serão, inegavelmente, parte do future, e esta crise global pode ser o ponto de viragem para ainda mais mudanças na maneira como a energia é produzida e aproveitada.

Para se atingir um futuro mais "verde", a luz solar é, provavelmente, a fonte de energia renovável mais conveniente; contudo, dada a sua natureza intermitente, o armazenamento da energia solar é necessário, e deve ter um ciclo de vida com um baixo impacto no ambiente. Células solares de escoamento mostram grande promessa na produção de energia térmica e elétrica em edifícios. Estes dispositivos combinam os princípios de funcionamento das células fotoeletroquímicas e redox de escoamento num único sistema. A célula fotoeletroquímica produz energia suficiente para ocorrerem reações redox, desta maneira convertendo energia solar em energia química, armazenada num combustível eletroquímico líquido armazenável, à semelhança da fotossíntese. Os eletrólitos também convertem a luz solar em energia térmica, que pode ser utilizada para conforto térmico e água sanitárias. A energia química armazenada pode ser facilmente e eficientemente convertida em eletricidade numa bateria redox de escoamento, que já é a tecnologia de baterias mais competitiva para aplicações estacionárias. Esta tecnologia encontra-se à escala laboratorial, e este trabalho pretende criar um caminho para a investigação futura e para a sua implementação industrial.

Foi realizada uma análise económica às células solares de escoamento para perceber o seu potencial para serem tecnicamente e economicamente viáveis. A viabilidade destes dispositivos só é possível se quatro requerimentos forem cumpridos simultaneamente: performance elevada, baixo custo, sustentabilidade e robustez. Este trabalho abrange comparações entre diferentes configurações do dispositivo (SRFC integrada, SRFC acopladas a painéis PV e SRFC com concentradores solares), condições de operação e combinações de materiais, dos quais, fotoelétrodos (hematite e vanadato de bismuto) e eletrólitos (ferrocianeto/antraquinona AQDS 2,7 e ferrocianeto/polioxometalato SiW_{12}), localizações (Portugal e Dinamarca) e escalas (instalações de 1 kW e 20 kW). O melhor cenário estudado para as células solares de escoamento foi baseado no uso de hematite como fotoelétrodo e nos pares redox ferrocianeto/AQDS como eletrólito, localizado na Dinamarca, e com uma instalação com 20 kW. Este cenário requer 2346 células fotoeletroquímicas para produzir 293,4 GWh em 20 anos (ideal para aplicação num bairro habitacional), tem um LCOE de 0,17 €·kWh^{-1} e um tempo de retorno de investimento de 11,2 anos, o que são valores comparáveis a um investimento em painéis fotovoltaicos e baterias de escoamento de vanádio para produzir a mesma potência.

Declaration

I hereby declare, under word of honour, that this work is original and that all non-original contributions is indicated and due reference is given to the author and source

Tiago Filipe Alberto Antunes

Porto, 3rd of July 2020

Index

List of Figures

List of Tables

Notation and Glossary

A	Area	m^2
C	Concentration Ratio	
CE	Columbic Efficiency	m
c_P	Thermal Capacity	$J \cdot K^{-1} \cdot kg^{-1}$
C_V	Volumetric Capacity	$A \cdot h \cdot L^{-1}$
DOD	Depth of Discharge	%
E	Energy	J
$\bar{E}_C$	Charging Potential	V
$\bar{E}_D$	Discharging Potential	V
E_d	Energy Density	$W \cdot h \cdot L^{-1}$
EE	Energy Efficiency	%
F	Faraday Constant	$C \cdot mol^{-1}$
G	Total Irradiation on a Surface	$W \cdot m^{-2}$
ΔH°	Redox Potential Difference Between Active Redox Pairs	V
$h_{c,g-a}$	Coefficient of Heat Transfer by Convection Between Glass and Air	$W \cdot K^{-1} \cdot m^{-2}$
$h_{r,g-a}$	Coefficient of Heat Transfer by Radiation Between Glass and Air	$W \cdot K^{-1} \cdot m^{-2}$
I	Incident Radiation	$kWh \cdot m^{-2}$
J	Current	A
j	Current Density	$mA \cdot cm^{-2}$
M	Molar Mass	$g \cdot mol^{-1}$
m	Mass	kg
$\dot{m}$	Mass Flow	$kg \cdot s^{-1}$
N	Amount of Redox Pairs	mol
n	Number of Electrons	
P	Power	W
Q	Material Flow	$mol \cdot s^{-1}$
Q_C	Charge Generated in the Charging Phase	C
Q_D	Charge Generated in the Discharging Phase	Cm
Q_R	Coefficient of Heat Transfer by Radiation	W
Q_u	Power Transferred	W
T	Temperature	K
t	Time	s
T_a	Temperature of Air	K
t_D	Time of Discharge	s

T_g	Temperature of Glass	K
T_{in}	Inlet Temperature	K
T_{out}	Outlet Temperature	K
U	Electrical Potential	V
U_L	Global Coefficient of Heat Transfer	$W \cdot K^{-1} \cdot m^{-2}$
V	Volume	m^3
VE	Voltage Efficiency	%

Greek Letters

α	Absorbance	%
ε	Emissivity	%
σ	Stefan-Boltzmann Constant, $5.670 \cdot 10^{-8}$	$W \cdot m^{-2} \cdot K^{-4}$
τ	Transmittance	%

Indexes

$_D$	Discharge
$_C$	Charge
$^\circ$	Standard

List of Acronyms

DSSC	Dye Sensitized Solar Cell
FTO	Fluorine Doped Tin Oxide
IPCE	Incidence Photon-to-Electron Conversion Efficiency
LCOE	Levelized Cost of Energy
LCOS	Levelized Cost of Storage
O&M	Operation and Maintenance
OCP	Open Circuit Potential
PEC	Photoelectrochemical
PEC-PV	Photoelectrode-Photovoltaic
PSC	Perovskite Solar Cell
PV	Photovoltaic
RES	Renewable Energy Sources
RFB	Redox Flow Battery
SOC	State of Charge
SRFC	Solar Redox Flow Cell
STCE	Solar-to-Chemical Conversion Efficiency
STH	Solar-to-Hydrogen
VRFB	Vanadium Redox Flow Battery

1 Introduction

1.1 Framing and presentation of the work

The greenhouse effect is a naturally occurring phenomenon on Earth. Gases in the atmosphere trap infrared radiation close to the Earth's surface; this radiation is responsible for maintaining the average temperature of the Earth's surface at *ca.* 14 ºC. [1] The greenhouse effect is one of the main reasons that enable the existence of life on our planet.

The discovery of fossil fuels (coal, oil, natural gas) and the creation of ways to harness their power plays a dominant role in global energy systems. Even though fossil energy was a fundamental driver of the Industrial Revolution, and the technological, social and economic progress that has followed, it also brought some terrible consequences. In the last century, mainly through the burning of fossil fuels, humans have been interfering with the energy balance of the planet, which give off additional carbon dioxide into the air.[1,2] Analyzing Figure 1.1, it becomes clear that the level of carbon dioxide in the Earth's atmosphere has been rising consistently for decades and traps extra heat near the surface of the Earth, causing temperatures to rise – global warming.

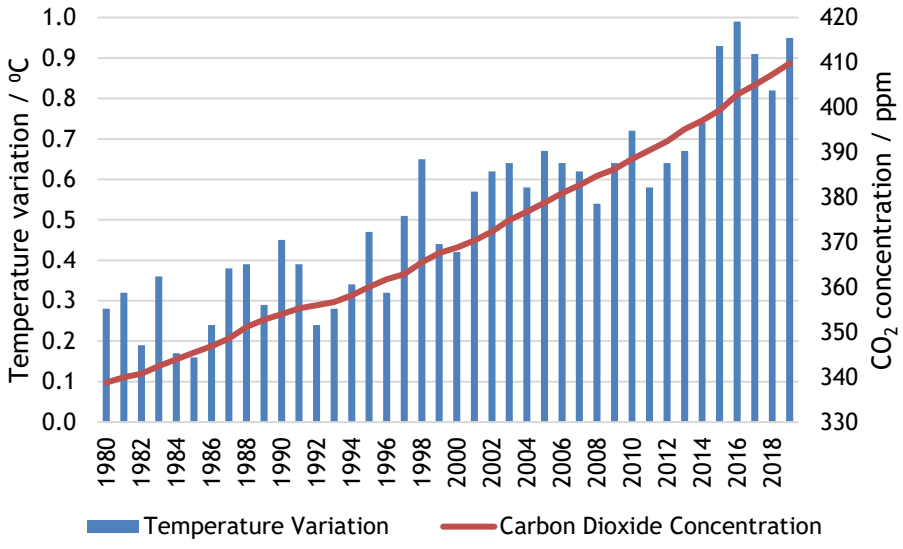

Figure 1.1 – Variation of temperature in the surface of the Earth and concentration of carbon dioxide in the atmosphere from 1980 to 2018, global temperature is averaged and adjusted to the 20th century average. (Adapted from NOAA)[3,4]

Renewable energy sources are the best alternative for the world current dependence on fossil fuels, giving a substantial contribution for the energy decarbonization. The renewable sources,

such as solar, wind, wave energies and hydropower, are clean, abundant and do not emit greenhouse gases or other pollutants. Renewable power is growing at incredible rates, i.e. it accounted for 72 % of all power expansion in 2019, according to the International Renewable Energy Agency's (IRENA) Renewable Capacity Statistics 2020. The global renewable energy increased by 7.6 % in 2019, accounting for 2.537 gigawatts (GW) of generating capacity - Figure 1.2. Solar energy lead renewable capacity expansion with 586 GW, corresponding to an increase of 20 %, followed by wind energy increased by 10 %.[5] On the solar sector, photovoltaic (PV) capacity had a 78 % worldwide increase from 2014 to 2018.

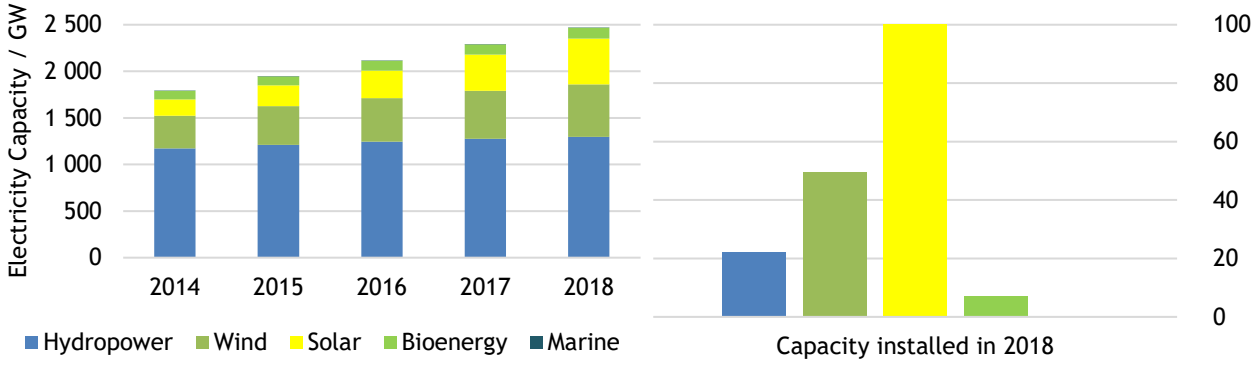

Figure 1.2 – Growth of renewable energy capacity in the world, from 2015 to 2018, and total electrical capacity installed in 2018. (Adapted from IRENA)[5]

Portugal follows the same trend as the rest of the world. Renewable energy is the fastest growing source of electricity supply, corresponding to 52.6 % in 2018[6], and solar and wind energies continued to dominate. Portugal presents one of the biggest PV power potentials in Europe, as shown in Figure 1.3, mainly due to its extensive coast and great solar exposure. Nevertheless, harnessing the full potential of the Sun is still challenging.

Sunlight is probably the most abundant and convenient renewable energy source available in our planet for producing *in-loco* thermal and electrical energy. PV cells can produce electricity with the needed scalability; only 0.16 % of the Earth's surface area needs to be covered with 10 % efficient solar cells to fulfill the humankind energy consumption of *ca.* 20 TW.[7] However, this technology, like all other solar powered technologies, has a problem, it only works during the day and in sunny days, requiring storage solutions. The cost of the PV/storage electricity is already lower than the grid electricity for some EU countries such as Denmark, Germany, Italy, Portugal and Spain, but still expensive and does not address inter-season storage.[8]

Photoelectrochemical (PEC) cells provide an alternative platform for converting sunlight into storable fuels (mimicking photosynthesis) easily convertible into electricity. While originally the research on PEC cells targeted the solar hydrogen production, scientists are still struggling to develop a viable PEC system mostly because of the fixed energy levels imposed by the water splitting reaction that often do not match the ones of the semiconductors used.[9] PEC cells have also been considered for the carbon dioxide reduction; however, this approach faces, unless hydrogen is used, the same challenges of water splitting.[10]

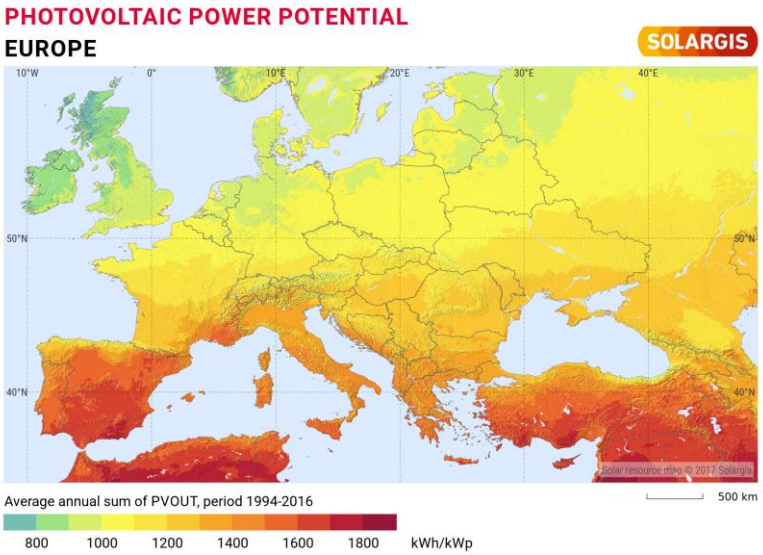

Figure 1.3 - Photovoltaic power potential in Europe. (Source: Solar resource map © 2019 Solargis)[11]

In parallel with the exploitation of renewable electricity generation technologies, the most used and viable way for very large-scale energy storage is, nowadays, in pumped hydroelectric energy storage.[12] The production of hydrogen through electrolysis is also an option that is being studied to solve this problem. Even though these are great solutions for very large-scale energy storage, batteries showed great potentials as reliable systems that can store, supply, modulate, and transport electricity. For large-scale stationary storage systems, high storage capacity is often required. Redox flow batteries (RFBs) demonstrated great advantages when compared with other electrochemical devices: high degree of customization to meet specific power and energy needs separately, scalability and lower cost. The energy is stored in fluid electrolytes and the storage capacity is determined by the redox pairs, the volume and concentration of electrolyte (*i.e.* the size of the tanks storing the electrolytes), while the power output depends on the electrode area and current density (*i.e.* the size of the electrochemical cells stack).[9] The most matured RFB technology with larger commercial penetration uses vanadium redox pairs in a sulfuric acid aqueous electrolyte[13], but new organic RFB are being designed to offer longer duration, as well as higher power and energy densities, in a more environmentally sustainable format. One of the goals of this technology is to provide cost-effective multi-seasons energy storage; the RFBs are already the most competitive battery

technology for stationary application with forecasted levelized cost of storage (LCOS) of 3 ¢€·kWh^{-1} per charging cycle by 2050.[14] The combination of solar energy storage and conversion into electrical energy seems to be the best solution for off-grid solar electrification.[15]

A solar redox flow cell (SRFC) consists of a PEC cell to charge electrochemical redox pairs in the liquid phase, which will be discharged at a RFB to produce electricity.[16] The SRFC device presents a unique advantage of allowing the cogeneration of electrochemical and thermal energies; the latter serves for thermal comfort and for sanitary waters. Figure 1.4 depicts the implementation of this technology in a house. The SRFC technology is very flexible and cost-competitive and it is expected to give a substantial contribution for the energy decarbonization especially when used in buildings assisting them to become nearly zero-energy buildings (NZEB) - European Directive (2018/844).[17] However, it is important to note that SRFCs are still at a scientific research stage and not ready for commercialization. The performance of SRFCs is far from economically or technically satisfactory due to the intrinsic efficiency limits of the solar energy conversion components, *i.e.* the semiconductors, and the working chemical potential mismatch between the solar and electrochemical energy components.

Breakthrough discoveries that show a SRFC displaying simultaneously a solar conversion efficiency of > 10 %, stability for > 10 years, high energy density and scalability need to be addressed. Moreover, a techno-economic modeling to outline performance targets, in terms of *e.g.* raw material costs (semiconductors, redox pairs, membrane, supporting electrolyte), device design, system configuration and operating conditions, are also a tiebreaker for fast technology development. These studies were performed for more mature PEC and RFB technologies, but for SRFCs have not been performed.[18] This thesis aims to provide a detailed cost analysis for SRFCs and support the materials choice and design guidelines for a practical approach to competitive solar fuel production in the future.

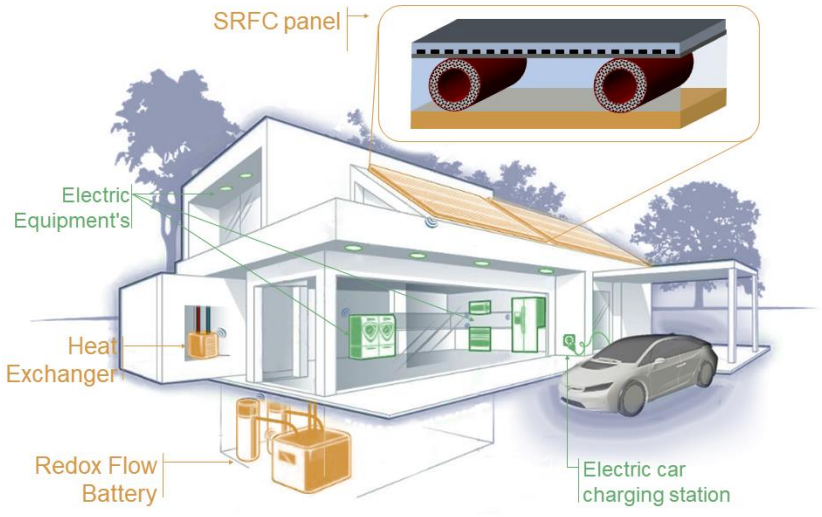

Figure 1.4 - Conceptual sketch of a SRFC application on the roof, combining a RFB and a heat exchanger on the basement for solar-to-output electricity and thermal energy conversion, respectively.

1.2 Contribution of the author to the work

Solar redox flow cells have been in development for some years, however it has not been reported any economic analysis towards this technology. The economic analysis made in this work aims to give some insights in the major drawbacks of the SRFC technology, as well as, its best properties. It also will show the best materials to be implemented in this technology from an economic standpoint and give a perspective of how far it is to be a commercial technology.

1.3 Organization of the thesis

Chapter 1 – Introduction

One of humanity's biggest problems is presented, global warming. This has caused the World to reduce its carbon footprint, mainly by finding "green" ways to produce energy. A context of the contemporary energy situation is given, highlighting renewable sources, in particular the role of solar energy to supply the current global energy demand and environmental sustainability. The main problems related to solar energy harvesting and storage are exposed, and the SRFCs are introduced as a promising technology to mitigate these problems.

Chapter 2 – Context and State of the Art

Insights into the working principles and components of SRFCs were given. Recent research about SRFC device configurations, photoelectrodes and electrolytes were summarized and some of the best results were presented.

Chapter 3 – Materials and Methods

In this section, a description of the different SRFC arrangements studied in this work in terms of materials, location and scalability was presented in detail, as well as the prices and assumptions made for the economic analysis. The formulas used for the analysis were described and explained.

Chapter 4 – Results and Discussion

The main results obtained in the economic analysis were presented and discussed in this chapter to conclude about the best combination of materials for the photoelectrodes and redox pairs/electrolytes, the effect of different locations and scalability to turn SRFCs profitable.

Chapter 5 – Conclusions

Summarizes the work developed during this thesis, relating the main conclusions achieved.

Chapter 6 – Assessment of the work done

In this chapter, a reflection was made on the work developed, and suggestions for future work in the domain of the theme developed in the present master thesis were presented.

2 Context and State of the Art

The utilization of solar energy demands not only efficient energy conversion but also inexpensive energy storage to make it dispatchable. Although connecting PVs with batteries, as adopted by some solar farms nowadays, can provide the same uninterrupted power supply, the high capital cost and large footprint of two separate devices limit the market cases feasible for this option.[19] In contrast, solar redox flow cells (SRFCs) promise to be efficient and cost-effective standalone energy systems for sustainable off-grid electrification.[15] Properly designed SRFC devices can be charged under sunlight illumination without any external electric bias and deliver a high energy density comparable to that of state-of the-art RFBs over many cycles.

SFRCs still present some problems that invalidate them as a viable technology:[15]

- The necessity of accurately matching the semiconductor bandgap energy with the thermodynamic potential of respective redox reaction
- Low solubility of active materials in the electrolyte, which results in a low energy density;
- It is still difficult to achieve high state of charge of the electrolyte using photocharging without bias;
- Low solar-to-chemical and solar-to-electrical energy conversion efficiencies;
- Low discharge current densities.

Both PECs and RFBs have been investigated for more than three decades, yet the integration of these two systems has not reached maturity. Hence, the present dissertation aims to give a critical overview of the state-of-the-art progress in SRFCs, from the aspects of the working mechanism, materials choice, device engineering, and performance evaluation. Moreover, a detailed cost analysis was performed to provide important guidelines for choosing device components and optimizing design and operating features required to turn this technology cost-competitive with current generation ones.

2.1 Solar Redox Flow Cells (SRFCs) – Working Principles

Solar redox flow cells combine two technologies: a photoelectrochemical cell for sunlight harnessing into electrochemical and thermal energies and a redox flow battery to easily and efficiently convert chemical energy into electricity. At a SRFC, the electrochemical redox pairs in the liquid phase are photocharged in the PEC cell, based on the formation of a photoelectrode-electrolyte junction, which are then discharged in the RFB cell, producing electricity. Figure 2.1 demonstrates a schematic of a SRFC.

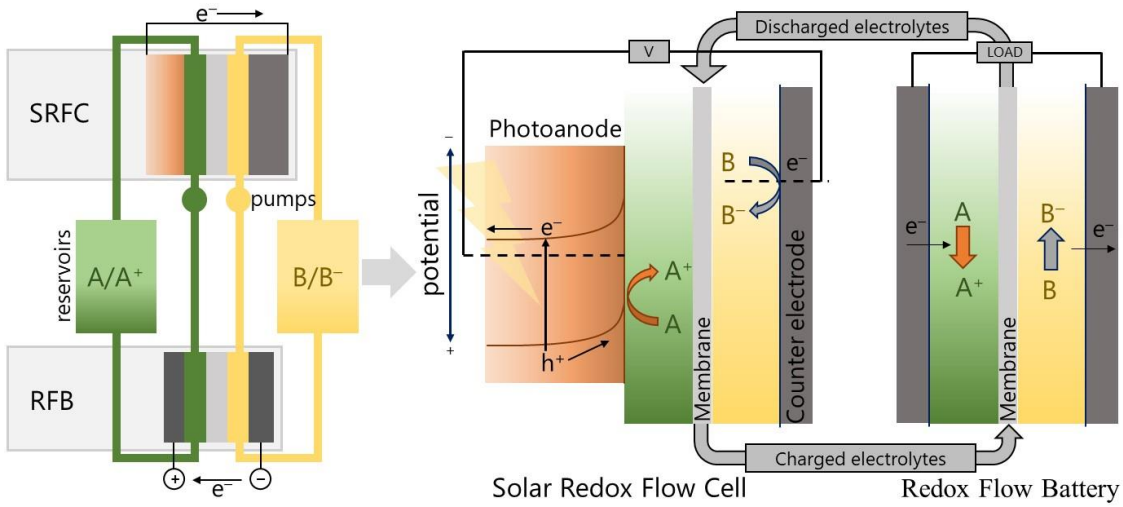

Figure 2.1 - Representative scheme of a solar redox flow cell (SRFC) equipped with a photoanode. The output could be split between charging the redox flow battery (RFB) system during daylight and discharging the battery in the dark (A/A^+ and B/B^- are the redox pairs of positive and negative electrolytes, respectively). (Adapted from: Proceedings of nanoGe Fall Meeting19)[20]

Becquerel was the first person to perform a photoelectrochemical experiment in 1839, demonstrating that it was possible to create a voltage and electric current using a light source. The Becquerel effect, as it is called, happens when there is a semiconductor-electrolyte junction, in a solid-electrolyte interface. This interface enables the transfer of charge carriers (electrons in n-type semiconductors and holes in p-type semiconductors) to the electrolyte, driven by the difference in Fermi levels between the two phases (E_F). The charge transfer creates a thermodynamic equilibrium and equalizes the Fermi levels. When this effect is produced from the illumination of the junction, it is called photovoltaic response.[21]

The simple configuration of a PEC cell consists of a single photoelectrode and a dark counter electrode, both immersed in an electrolyte solution that allows the transport of ionic species and separated by an ion conductive membrane. The photoactive material can be either an n-type or p-type semiconductor. A semiconductor having large number of electrons in the conduction band is an n-type semiconductor (photoanode), whereas in a p-type semiconductor (photocathode) the holes are the majority carriers. In the case of a n-type semiconductor, if the initial Fermi level of this phase is higher than the initial Fermi level of the electrolyte, the equilibrium between these two levels is achieved by the movement of electrons from the semiconductor to the electrolyte. This process creates a layer in the semiconductor with positive charge, a depletion layer (w). To avoid the transfer of electrons to the electrolyte, a potential barrier is created by the bending of the valence and conduction band edges. This effect is shown in Figure 2.2 (left side). In the case of p-type semiconductors, the effect is inversed.[21]

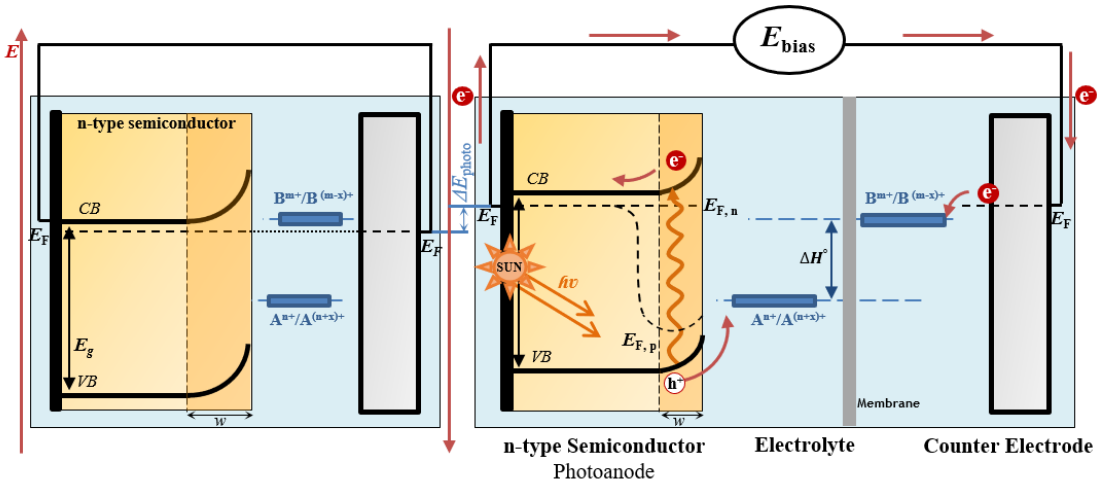

Figure 2.2 - Energy diagram of a PEC cell. (Adapted from: Dias e Mendes, 2018)[22]

Under illumination, when the semiconductor absorbs photons (hv) with energies greater than its bandgap, electron-hole ($e^- - h^+$) pairs are created - in Figure 2.2 (right side). In the depletion layer these pairs are separated by the electric field that has been generated in the semiconductor-electrolyte junction. This results in a shift in the semiconductor's Fermi level toward its original value, before the establishment of the semiconductor-electrolyte junction, which means that the illuminated semiconductor's potential is closer to its flat band potential.[21]

The photovoltage created between an illuminated semiconductor and a metal counter electrode, in an open circuit condition, is equal to the difference between Fermi levels in the redox potential of the electrolyte and the semiconductor. When the circuit is closed, there is no photovoltage because the Fermi levels are equaled. Nonetheless, the illumination generates minority charge carriers in the semiconductor, which cause redox reactions of chemical species in the electrolyte - Equation 2.1 is the half reaction that occurs in the anode, Equation 2.2 is the half reaction of the cathode and Equation 2.3 is the overall reaction of the PEC device.

$$A^{n+} \rightarrow A^{(n+x)+} + xe^- \qquad 2.1$$

$$B^{m+} + xe^- \rightarrow B^{(m-x)+} \qquad 2.2$$

$$A^{n+} + B^{m+} + hv \rightarrow A^{(n+x)+} + B^{(m-x)+} \qquad 2.3$$

In n-type semiconductors, the minority charge carriers are holes, which cause anodic oxidation reactions and in p-type semiconductors, electrons are the minority charge carriers, causing cathodic reduction reactions. At the same time the majority charge carriers leave the semiconductor through an external circuit into the counter electrode. In this electrode the charge carriers force a redox reaction inverse to the one occurring in the semiconductor. [21] To achieve unbiased solar charging of redox flow cells, the potentials of the redox pairs of the electrolytes need to match the bandgap energy (difference between the valence band potential and conduction band potential) of the semiconductor.

A RFB is an electrochemical device where two redox pairs dissolved in a liquid electrolyte are used to easily store energy that is efficiently convertible into electricity. This technology handles power and storage capacity separately; the power is related to the size of the electrochemical cells stack, while the capacity is related to the size of the tanks storing the electrolytes. The vanadium RFB (VRFB), first proposed by Skyllas-Kazacos in the 1980s, is the most mature technology, already with commercial applications.[13] The electrode reactions during the charge stage are: $VO^{2+} + H_2O \rightarrow VO_2^+ + 2\ H^+ + e^-$; E^0 = -0.99 V_{SHE} and $V^{3+} + e^- \rightarrow V^{2+}$; E^0 = -0.26 V_{SHE}. Since these reactions, as for most of the selected redox pairs, involve just one electron exchange, the electrodes are normally of carbon felt and the overpotentials are quite small. Due to their unique advantages, in 2018 more than 92 multi-kW or MW all-vanadium RFBs were under contract, construction, or operation around the world.[15] Other chemistries are now emerging for RFBs, *e.g.* aqueous organic redox couples and inorganic polyoxometalates (POMs),[23] targeting higher energy densities and displaying lower overall cost.

The concept of SRFCs was first demonstrated in 1976 by Hodes *et al.*[24] and stayed dormant until 2013;[25] however, in only seven years, the efficiency of SRFCs reached integrating III-V tandem junction solar cells with properly voltage matched RFBs.[26] Although III-V semiconductors can enable unprecedented high performance, only ten photocharging cycles were demonstrated, which together with the excessive manufacturing cost turn this device unpractical. For thermal harvesting and scalability purposes, an integrated SRFC is more suitable than the PV-charged RFB, but efficiencies < 5 % were reported so far using single photoelectrodes.[27] Moreover, using sunlight to heat up the electrolytes, it is possible to take advantage of the 80-85 % of the solar energy that is not converted into electrochemical energy.[9] The heat stored in the electrolytes can then be heat-exchanged for sanitary water applications or for thermal comfort, which increases the overall efficiency of the system.[28]

Research in the field of SRFCs is currently focused on the development of high performance photoelectrodes and redox couples whose energy-level matching should allow for an unbiased and highly efficient photocharge. The semiconductor materials need to be simultaneously efficient, stable, Earth-abundant and produced by low-cost techniques and the redox couples/electrolytes need to have a high energy density (high solubility), low ionic resistance and fast kinetics.[15] The development of tandem photoelectrodes, such as photoanode-photocathode and photoelectrode-photovoltaic (PEC-PV) configurations, are capable of higher photopotentials, and then driving redox reactions with higher potential difference. PEC-PV tandem photoelectrode demonstrated already efficiencies for water splitting similar to commercial PV-assisted devices;[29] Si solar cells and emergent perovskite and dye sensitized solar cells (PSCs and DSSCs, respectively) are promising PV cells for such configuration. Table 2.1 presents a summary of the best SRFC reported to date.

Table 2.1 – Representative demonstrations of SRFCs reported in literature based on single and tandem photoelectrodes. Photoelectrodes are highlighted in bold.

Anodic half-cell	Separator	Cathodic half-cell	Performance	Ref
CdS/DSSC tandem | 0.4 M VO^{2+}/VO_2^+ in 2 M H_2SO_4	Nafion 117	0.4 M V^{3+}/V^{2+} in 2 M H_2SO_4 | Carbon felt	Photocurrent of 1.4 mA·cm^{-2} without external bias Photopotential 1.3 V	[30]
n-Si | 0.2 M Br_3^-/Br^- in 1 M H_2SO_4	Nafion 115	**p-Si** | 0.5 M AQDS/$AQDSH_2$ in 1 M H_2SO_4	Solar-to-chemical conversion efficiency of 5.9 % Photopotential 0.8 V Discharge capacity 730 mA·h·L^{-1}	[31]
Polyaniline-coated α-Fe_2O_3 | 0.2 M $Fe(CN)_6^{4-}$ / $Fe(CN)_6^{3-}$ in 1 M NaOH	Nafion 117	0.1 M 2,7-AQDS/ 2,7-$AQDS^{2-}$ in 1 M NaOH | Graphite felt	Photocurrent of 0.14 mA·cm^{-2} without external bias Photopotential 1.3 V Photocurrent of 0.10 mA·cm^{-2}	[32]
Ta_3N_5 |0.4 M $Fe(CN)_6^{3-}$/ $Fe(CN)_6^{4-}$ in 1 M KOH	Nafion 212	**p-Si/GaN tandem** | 0.1 M 2,6-DHAQ/ 2,6-reDHAQ in 1 M KOH	Solar-to-chemical conversion efficiency of 3.0 % Photopotential 1.4 V	[33]
n-WSe_2 | 0.2 M I_3^-/I^- in 0.5 M H_2SO_4	Nafion	10 mM AQS/$AQSH_2$ in 0.2 M NaI and 0.5 M	Overall roundtrip efficiency of 2.8 %	[34]
InGaP/GaAs/Ge PV or Carbon felt | 0.1 M 4-OH-TEMPO$^+$/4-OH-TEMPO in 2 M NaCl	FAA-3-50	0.1 M MV^{2+}/MV^+ in 2 M NaCl | Carbon felt	Solar-to-output energy conversion efficiency of 14.1 % Photopotential 2.4 V	[26]
Graphite felt | 0.4 M TEMPO-SO_4^- in 1 M NH_4Cl	Nafion 117	**p-Si protected with TiO_2 and Pt** | 0.4 M $Fe(CN)_6^{3-}$/ $Fe(CN)_6^{4-}$ in 1 M NH_4Cl	Solar-to-chemical conversion efficiency of 1.6 % Energy density 3.9 W·h·L^{-1} from 0-95 % SOC	[35]
WO_3-decorated $BiVO_4$ | Br_3^-/Br^- in 0.5 M H_3BO_3	Nafion 211	0.2 M I_3^-/I^- in 0.5 M H_3BO_3| Carbon felt	Solar-to-output energy conversion efficiency of 1.3 % Photocurrent decrease from 4.2 to 3.2 mA·cm^{-2} during 1 h Solar-to-chemical conversion efficiency of 1.9 %	[36]
Bare α-Fe_2O_3/DSSC tandem | 0.25 mM I^-/ I_2 in 1 M NH_4I	Nafion 212	0.25 M 2,7-AQDS/ 2,7-$AQDS^{2-}$ in 1 M NH_4I | Carbon feltarbon felt	Solar-to-chemical conversion efficiency of 0.1 % Photopotential 1.6 V	[37]
n^+np^+-Si/Ti/TiO_2/Pt or Carbon felt | 0.2 M BTMAP-Fc in 1 M NaCl	Selemion DSV	0.2 M BTMAP-Vi in 1 M NaCl | **p^+np^+-Si/Ti/TiO_2/Pt** or Carbon felt	Solar-to-output energy conversion efficiency of 5.4 % Photopotential 1.1 V	[38]

2.2 Photoelectrodes

The photoelectrode is the main component of a PEC device. It is responsible for the generation of photocurrent and photopotential, assuming a key role in the overall SRFC performance. Therefore, the photoelectrode has to fulfil several requirements for an efficient solar fuel production: i) the bandgap energy needs to be aligned with the redox potential of the redox pairs/electrolyte[39]; ii) needs to be chemically stable, essential to guarantee a long life-time of the device[15]; iii) needs to have good charge carrier mobility to ensure fast reaction kinetics[39]; and iv) must be low cost and Earth-abundant.[40] The search for a semiconductor material with these characteristics has extended for some time now, which made way for the discovery of many semiconductors. Figure 2.3 has some of the most promising materials and their respective band gap.

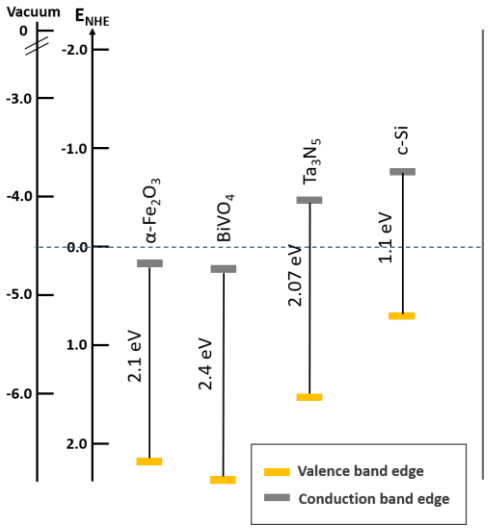

Figure 2.3 – Photoelectrodes and their respective band gap alignment. (Adapted from: Zhou et al., 2018)[36]

This work aims at the use of n-type metal-oxide semiconductors for SRFCs, such as hematite (α-Fe_2O_3) and bismuth vanadate ($BiVO_4$), extensively studied for PEC cells mainly due to their abundance, high theoretical photocurrent (>12 $mA \cdot cm^{-2}$), stability and scalability. α-Fe_2O_3 photoelectrode is the material of excellence developed at LEPABE's group, which reported the most stable flat thin film ever reported and the highest photopotential with $IrO_2/RuO_2/\alpha$-Fe_2O_3 for PEC water splitting applications.[40,41] Moreover, this group also developed the first alkaline SRFC based on stable α-Fe_2O_3 photoelectrode coupled with ferrocyanide/AQDS,[32] and more recently with iodide/AQDS.[37] On the other hand, $BiVO_4$ photoelectrode is not produced at LEPABE despite the promising achievements for solar water splitting and solar charging redox flow cells.[36] Therefore, this work plan initially aimed at the preparation and optimization of $BiVO_4$ using spray pyrolysis, a reproducible and easily scalable technique. A detailed state-of-the art of $BiVO_4$ photoelectrode was performed and is described in the following sub-sections.

2.2.1 Bismuth Vanadate ($BiVO_4$)

This semiconductor material has great potential as a photoanode, in fact, it is one of the most promising materials that has been used for the production of solar fuels. Bismuth Vanadate has a direct band gap of 2.4 eV, which is translated to a theoretical maximum solar-to-hydrogen (STH) conversion efficiency of 9.2 %. Photocurrent densities as high as 6.7 mA/cm^2 at 1.23 V_{RHE} in nanostructured heterojunction samples were reported using tungsten trioxide (WO_3) nanorods as scaffolds for the $BiVO_4$ top layer with cobalt phosphate (Co-Pi) surface modification.[42] Combining this material with a GaAs/InGaAsP PV cell, in a PEC-PV tandem configuration, allowed to achieve a higher solar-to-fuel of 8.1 %; this value corresponds to one of the highest ever reported for solar to fuel production. When cheap c-Si PV cells were combined with $BiVO_4$ a maximum efficiency of 7.7 % was reported.[43] Regarding stability, this photoanode material shows a reasonable stability in neutral pH electrolytes (3-10), such as bicarbonate (HCO_3^{2-}), borate (BO_3^{2-}) and phosphate-based electrolytes (PO_4^{3-}, HPO_4^{2-} and $H_2PO_4^-$). $BiVO_4$ is easily corroded with illumination, high applied bias and alkaline electrolytes (pH 6.8-14).[39] Other attractive characteristic of $BiVO_4$ photoelectrode is its synthesis employing low-cost and scalable deposition techniques based on solution processing, such as spray pyrolysis. This allowed to construct the largest PEC-PV device ever reported with an impressive 1.6 m^2; however, the efficiency of this system was not reported.[44]

The strategies that have been used to improve the performance of $BiVO_4$ photoelectrodes are:[39]

- Heterojunctions to create an electron transfer junction and improve the light harvesting capabilities of $BiVO_4$, which translates in higher bulk and surface efficiencies.
- Doping with certain impurities to improve the lifetime and n-type conductivity in the bulk, and the active sites in the surface.
- Post treatment at high-temperatures to induce above post synthetic defects, which can improve the bulk and surface efficiencies.
- Addition of an electrocatalyst and/or hole transfer layer to reduce the surface charge recombination and prevent corrosion.

2.2.2 Strategies to Improve Semiconductor Performance

Heterojunctions

To form an effective heterojunction, the material used should have better electron transfer capacities than $BiVO_4$. Tungsten oxide (WO_3) is a good example, which has already been accomplished with great results. The $BiVO_4/WO_3$ junction also partially dopes the bismuth semiconductor material with tungsten, which further improves the performance of the

photoanode. Tin oxide (SnO_2) is another promising material to combine with $BiVO_4$, also preventing the hole transfer toward the defects of the fluorine doped tin oxide (FTO) glass.[39]

Doping

$BiVO_4$ has slow majority carrier transfer kinetics, which means that the addition of a dopant is very important to improve the performance of the photoelectrode. Doping of intrinsic defects in the $BiVO_4$ structure with a n-type dopant, such as tungsten (W) and molybdenum (Mo), enhances the semiconductor conductivity, charge separation and transfer efficiencies, culminating in improved performance behaviors.[39]

Post treatment

The treatment of photoelectrodes with hydrogen (H_2) and nitrogen (N_2) create oxygen vacancies in the $BiVO_4$ lattice. These treatments reduce the metal oxide and surface defect state, which increases the number of charge carriers and induces possible passivation. The N_2 treatment alters the optical properties of the photoelectrode, a redshift occurs in the bandgap from 2.5 eV (496 nm) to 2.3 eV (539 nm) while also extending the absorbance and effective incidence photon-to-electron conversion efficiency (IPCE) response.[39]

Electrocatalyst and hole transfer layer

Catalysts and hole transfer layers are normally used to reduce the overpotential, increase the semiconductor stability and improve the generated photocurrent. Co-Pi catalyst is one of the most effective materials used with $BiVO_4$. This catalyst reduces the hole transfer rates to the electrolyte but compensates this effect by reducing the electron-hole recombination rate. Although the advantages of using Co-Pi are quite attractive, the catalyst does not present great stability. To increase the stability of the photoelectrode a NiOOH/FeOOH double-layer catalyst was reported showing stable behavior over 50 h.[39] Moreover, using an in-situ catalyst regeneration process, which ensures selective NiFe catalyst re-deposition, a stable operation for > 1000 h were reported by Kuang *et al*.[45]

2.3 Electrolytes

For designing an efficient and stable SRFC, it is critical to understand not only its working principles, based on the physics of semiconductors and the thermodynamics of semiconductor-liquid interfaces, but also good compatibility among the redox pairs, electrolytes and semiconductors. The energy level alignment of the redox potentials and band edges of the semiconductors dictates the charge extraction, recombination and photopotential in the final system, and a suitable choice of the supporting electrolyte will enhance stability of both the semiconductor and the redox couples. For RFB systems, the active species are the redox couples dissolved in the supporting electrolyte solutions (hereafter denoted redox electrolytes); the

redox active cathode and anode materials are then named as the catholyte and anolyte, respectively. The separator is permeable to the supporting electrolyte (a conducting salt), but impermeable to the redox couples. Nowadays, there are already more than 1000 redox pairs identified as candidates for using in RFBs.[46]

The donor (D/D^+) and acceptor (A/A^-) redox pairs must satisfy a number of requirements for SRFC applications:[15]

i) fast redox reaction kinetic rates for high power density operation;
ii) high solubility (in a wide pH range) in the selected solvent for high energy density and high current density operation;
iii) sufficient formal potential window for high cell voltage, accurately matching the Nernst redox potentials with the semiconductor band edges to fully harvest the available photovoltage;
iv) good ionic conductivity for higher voltage efficiency;
v) low viscosity for reduced pumping energy consumption;
vi) high transparency within the photoelectrode absorption spectrum;
vii) stable, abundant, low-cost and environmentally safe features.

The electrical performance of a SRFC can be then measured by the following parameters:[20]

i) Volumetric capacity (C_V) – measurement of the maximum charge that can be stored in a fixed amount of electrolyte, usually presented in $A{\cdot}h{\cdot}L^{-1}$;
ii) Energy density (E_d) – measurement of the amount of energy that a fixed amount of electrolyte can store, presented in units of $W{\cdot}h{\cdot}L^{-1}$;
iii) Current density (j) – measurement of the amount of current generated by area of membrane, in units of $mA{\cdot}cm^{-2}$;
iv) Coulombic efficiency (*CE*) – quotient between the stored charge in the discharging phase (Q_D) and the charge generated in the charging phase (Q_C) of a single charge/discharge cycle;
v) Voltage efficiency (*VE*) – quotient between average discharging potential ($\bar{E}_D$) and the average charging potential ($\bar{E}_C$), using constant current;
vi) Energy efficiency (*EE*) – measurement of the applied and stored energy.

These performance indicators can be calculated using the following equations:

i) $$C_V = \frac{m \cdot n \cdot F}{M \cdot V} \qquad 2.4$$

ii) $$E_d = C_V \cdot U \qquad 2.5$$

iii) $$j = \frac{J}{A} \qquad 2.6$$

iv) $$CE = \frac{Q_D}{Q_C} \quad 2.7$$

v) $$VE = \frac{\bar{E}_D}{\bar{E}_C} \quad 2.8$$

vi) $$EE = CE \cdot VE \quad 2.9$$

*w*here *m* is the mass, *n* is the number of electrons, *F* is the Faraday constant, *M* is the molar mass, *V* is the volume, *U* is the electrical potential and *J* is the current.

Redox electrolytes can be divided by their phases, single phase and two phase, and by their type, aqueous and non-aqueous.[47] Only single phase electrolytes are of interest for this work and will be further analyzed. Recently, extensive research in aqueous organic and metal-organic complexes redox couples for RFBs has emerged; nevertheless, a fully organic or halogen/metal-organic and organic redox electrolyte combination is suitable for stable SRFCs, due to the low-cost, abundance, high reliability and tunable structure of organic redox couples.[48] Another type of aqueous-based redox electrochemistry uses inorganic redox couples, such as polyoxometalates (POMs). POMs form a class of discrete transition metal-oxide nanoclusters, being prepared from metals, but offering high structural diversity, fast redox kinetics and multi-electron transfer, due to their high capacity per molecule.[23] As a drawback, the aqueous electrolytes are limited by the redox potential of water: using redox pairs with potentials close to water's redox potential can result in electrolysis, which limits the maximum potential of the RFB, lowering the energy density.[48] On the other hand, non-aqueous electrolytes are not limited by water's redox potential, since they use organic solvents instead of water. They feature desirable properties such as: lower freezing and higher boiling temperatures, a much larger electrochemical stability window, *i.e.* 5 V instead of 1.2 V for water, and passive towards semiconductor corrosion. Despite the advantages of non-aqueous electrolytes, their high electrical resistance, low membrane selectivity, and (fire) safety concerns are limiting their commercial application.[19] Moreover, to date the aqueous systems are desired for the integration with a solar heating system. For these reasons, this thesis aims at the use of aqueous redox electrolytes and the most promising redox pairs will be further discussed.

2.3.1 Aqueous organic/metal-organic redox couples

Organic redox pairs are also a promising alternative in terms of environmentally friendliness. Guzik *et al.*[49] reported redox potentials and solubility values of 1710 quinones with potential usage in aqueous RFBs. The redox pairs show quasi-continuous redox potentials, from -0.8 V_{SHE} and 1.6 V_{SHE}, many with high aqueous solubility. Preference will be given to redox pairs with

suited redox potentials, matching the selected photoelectrode, fast kinetics, reversibility, high solubility, stability, low cost, safety and transparency.

Quinones, 2,2,6,6-tetramethylpiperidine-1-oxyl (TEMPO), alkoxybenzene and even polymers have become popular in SRFCs. Sulfonated anthraquinone species, such as AQDS (2,7), AQDS (2,6), and AQS (2), appear to be promising for the anode side (*i.e.* $E^0 > 0.50\ V_{NHE}$), while TEMPO is one of the most promising redox pairs for the cathode side.[20] Huskinson *et al.*[50] reported AQDS (2,7) with bromine in sulphuric acid, demonstrating equivalent efficiencies when compared to state-of-the-art RFBs. In fact, there is a large family of quinones that can be used with different redox potentials and pH tolerances.[51] Nonetheless, given the acidic nature of the electrolytes (pH~0), the photoelectrodes are still limited by their long-term stability. Very recently, the highest photocurrent ever reported for a SRFC was based on 4-OH-TEMPO/$MVCl_2$ redox couples, in neutral electrolytes, but only ten photocharging cycles were demonstrated.[26] The combination of ferrocyanide (metal-organic complex) in the positive side, together with quinones, has shown unprecedented electrochemical stability in organic flow batteries.[32] Therefore, it is most likely to identify stable neutral/alkaline flow battery chemistries based on metal complexes for the positive side, while the negative side could be organic based; in acidic solutions, metal ions can be used for the positive side too. Lin *et al.* published a 2,6-dihydroxyanthraquinone (2,6-DHAQ) (E^0 = -0.66 V_{NHE} at pH = 14) combined with potassium ferrocyanide (E^0 = 0.49 V_{NHE} at pH=13), displaying a high cell potential of 1.2 V.[51] Wedege *et al.* developed the first alkaline SRFC based on fast redox couples (ferrocyanide/AQDS) coupled with an extremely stable α-Fe_2O_3 photoelectrode.[32] Afterwards, these redox couples were used in a two-photoelectrode SRFC as well.[33] Recently, Li *et al.*[38] reported the long lifetime SRFC with >200 h under continuous operation based on highly stable BTMAP redox couples in neutral pH and Si photoelectrodes.

2.3.2 Aqueous inorganic redox couples

Inorganic redox couples are the most used in RFB electrolytes, in particular, metal redox couples. All-vanadium RFBs (VRFBs) are widely utilized and have been the subject of many studies over the years. Electrolytes using iron (Fe), chromium (Cr), zinc (Zn) and bromine (Br_2) are also commonly used.[20] However, these materials have shown in general problems related to the environmental and sociopolitical impact, acquisition costs, or the system design is too complicated for large-scale systems.

Polyoxometalates are new and emergent metal oxide molecules with a transition metal in its composition. POMs present good thermal stability, good conductivity, large surface areas, high solubility in water and other solvents, reduced permeability through cation exchange membranes and great redox properties. These materials are also non-toxic and non-volatile.[55] They are of great interest for SRFCs because of their multi-electron redox reactions and very

fast kinetics, which allow high current densities. POMs display electrochemical reaction kinetics 3-4 orders of magnitude faster than the vanadium system and are also expected to store *ca.* four times more energy than the standard all vanadium RFB.[23] Friedl *et al.*[52] reported two POMs for RFBs, $[SiW_{12}O_{40}]^{4-}$ and $[PV_{14}O_{42}]^{9-}$, that are stable over long term cycling (coulombic efficiency was 94 % during 155 cycles) and easily upscaled, *i.e.* a 1400 cm^2 POM-based RFB underwent over *ca.* 3 months, 1400 cycles, with no degradation of the redox systems and a negligible discharge capacity loss (the coulombic efficiency was 99.9 % and the energy efficiency 86 %). Pratt III *et al.*[53] designed a RFB using $[SiV^{V}_{3}W^{VI}_{9}O_{40}]^{7-}/[SiV^{IV}_{3}W^{VI}_{9}O_{40}]^{10-}$ and $[SiV^{IV}_{3}W^{VI}_{9}O_{40}]^{10-}/[SiV^{IV}_{3}W^{V}_{3}W^{VI}_{6}O_{40}]^{13-}$ in an aqueous electrolyte, presenting a coulombic efficiency bigger than 95 % during 100 cycles and an open circuit potential (OCP) of *ca.* 0.6 V. Chen, Symes and Cronin[54] tested $[P_2W_{18}O_{62}]^{6-}$ as anolyte in a RFB with HBr/Br_2 as catholyte, achieving coulombic efficiencies of 76 % with a concentration of 0.5 M of $[P_2W_{18}O_{62}]^{6-}$ in the electrolyte; this corresponds to an energy density of 225 $Wh{\cdot}L^{-1}$, and an OCP of 1.25 V. Feng *et al.*[55] constructed a RFB with 12-phosphotungstic acid and iodine as active species in the electrolyte, showing good stability, a coulombic efficiency of 99.6 % and an energy efficiency over 80.1 % in 700 charge/discharge cycles at a current density of 100 $mA{\cdot}cm^{-2}$.

It is expected that electrolyte cost will be two times cheaper using POMs made of abundant and cheap metals of manganese, nickel or iron (such as $Mn^{II/III}/Fe_{13}O_{40}$, $Mn^{III/V}/Fe_{13}O_{40}$, $SiMo_{12}O_{40}/Fe_{13}O_{40}$, $Mn^{II/III}/Al_{13}O_4(OH)_{24}(H_2O)_{12}$ and $Mn^{III/V}/Al_{13}O_4(OH)_{24}(H_2O)_{12}$).

3 Materials and Methods

As it was discussed in the previous chapter, a SRFC integrates in a single device a PEC cell and a RFB. In this work attention will be given to the photoelectrode materials and redox pairs/electrolytes, as well as their combination in the SRFC. The viability of such a device is only possible if four requirements are simultaneously fulfilled: high performance (efficiency and stability), low cost, sustainability, and robustness. All devices developed up to now provide combinations of these aspects but do not simultaneously fulfill all of them. Materials choice and device design guidelines outlining a pathway for scalable systems are required to provide a fast route to practical implementation.

The present thesis aims at developing a detailed cost analysis for solar energy conversion and storage using SRFCs, assessing their performance, manufacture and operation energy demand, but also balancing the use of cheap and/or expensive materials and device designs. Since SRFC technology is something new some assumptions were considered taking into consideration the available information of PECs and RFBs. Moreover, different scenarios will be studied, such as the use of PV panels and solar concentration devices known to push the technology with more ease into the market. The goal is to evaluate the cost of SRFC systems with power of 1 kW and 20 kW, reasonable range of values for solar home systems and neighborhood applications. This chapter focuses on the materials that will be considered and the assumptions made to make a realistic analysis.

3.1 Location

The location where solar technologies are installed is determinant for the energy that can be produced by them. With that in mind, two European countries were selected to make the economic analysis, Portugal and Denmark, one in the South and the other in the North. These two countries have different weather conditions, which makes them good choices for this work. In the context of this work, it was considered that the average annual solar global radiation in Denmark is *ca.* 1001 $kWh \cdot m^{-2}$ and in Portugal is *ca.* 1700 $kWh \cdot m^{-2}$.[56,57] Another key factor in the locations chosen is the price of electricity, which is 0.2984 $€ \cdot kWh^{-1}$ and 0.215 $€ \cdot kWh^{-1}$, in Denmark and in Portugal, respectively.[58]

3.2 Scale

Since this technology has the objective of being installed in a residence, it will be set two objective powers to be achieved with this technology, 1 kW and 20 kW. By comparing these two objectives, it will be possible to understand with bigger scales are advantageous or detrimental for the investment in SRFCs.

3.3 Photoelectrochemical Cell

The PEC cell is composed by two endplates, a photoelectrode compartment, one current collector that was treated in a gold bath, one Nafion 117 membrane, one graphite plate and one carbon felt electrode. Besides these main parts there is the need to use gaskets, o-rings and bolts to close the cell and ensure that there are no leakages. Figure 3.1 shows a schematic representation of all the components of the PEC cell (with an active area of 2 m^2) and their price are listed in Table 3.1 (based on the prices of the components at a laboratorial scale).

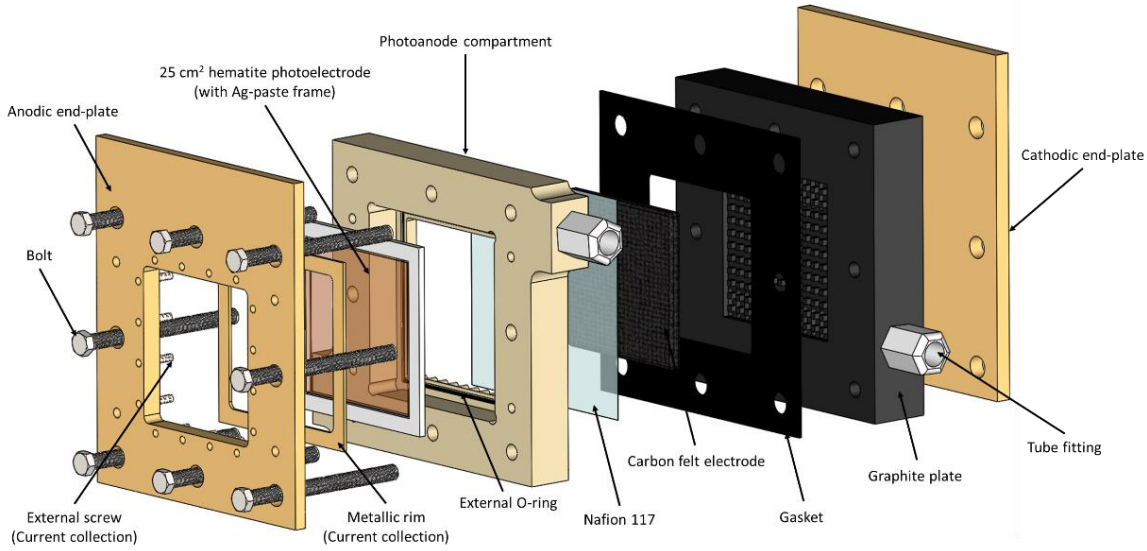

Figure 3.1 – Schematic representation of a 25 cm^2 PEC cell.

Table 3.1 – PEC components price.

Component	Price
Endplate	500 € per unit
Photoelectrode compartment	700 € per unit
Graphite plate	350 €·m^{-2}
Carbon felt	100 €·m^{-2}
Nafion 117	1700 €·m^{-2}
Current collector[59]	3000 € per unit
Bolts, gaskets and o-rings	150 € per unit
Tubes[59]	600 €·m^{-1}
Pumps[59]	64 €·h·m^{-3}
Assembly of the system	20 % of the investment
O&M	5 % of the investment

The photoelectrode is the key component in a PEC cell. The materials that will be the focus of this work are two stable and abundant metal-oxides: bismuth vanadate and hematite. $BiVO_4$ is a very promising semiconductor for PEC applications displaying > 90 % of its maximum theoretical efficiency, but there is only one work reporting its use in SRFCs with a solar-to-output energy conversion efficiency of 1.25 %.[36] On the other hand, α-Fe_2O_3 is the most stable metal-oxide ever reported and has been the target of some studies about its application in SRFC, however it has some problems in terms of performance (efficiencies of *ca.* 1 %).

It was considered that the production of these photoelectrodes is done by spray pyrolysis technique. For preparing the α-Fe_2O_3 photoelectrodes, the fluorine doped tin oxide (FTO) glass substrate is first pre-treated with a TEOS solution (10 % volume in ethanol) at 425 °C and air-annealed over 30 min, and then 42 mL of 10 mM solution of $Fe(acac)_3$ in EtOH was deposited for *ca.* 25 min. At the end, the samples were air-annealed for 30 min at 425 °C in the case of the larger photoelectrodes. The heating of the plate is considered to be constant and at a rate of 10 ºC·min^{-1}.[41] For the synthesis of $BiVO_4$, a $SnCl_4$ solution is firstly deposited at 425 ºC. The plate is then heated to 450 ºC and a solution containing $Bi(NO_3)_2{\cdot}5H_2O$ and $C_{10}H_{14}O_5V$ [$VO(acac)_2$] is deposited during *ca.* 200 min, finishing with air annealing for 2 h. The constant rate of the heating of the plate is 10 ºC·min^{-1}. Taking this information into consideration, the precursor solutions that are used for preparing the photoelectrodes with an active area of 25 cm^2 cost 84.3 €·m^{-2} and 1073 €·m^{-2} for α-Fe_2O_3 and $BiVO_4$, respectively; considering that the price of the FTO glass substrate is 584 €·m^{-2}. Since the plate is heated by 4 resistances of 350 W each, a total power of 1400 W, the energy expenditure in the production of the photoelectrodes amounts to *ca.* 1288 MWh·m^{-2} and 3416 MWh·m^{-2} for α-Fe_2O_3 and $BiVO_4$, respectively.

It was assumed that each PEC cell has an active area of 2 m^2 (made of 800 small cells of 25 cm^2) and that α-Fe_2O_3 works with a photocurrent of 0.65 mA·cm^{-2} and $BiVO_4$ with a photocurrent of 3.6 mA·cm^{-2}, which are the values reported in the literature for these photoelectrodes produced by spray pyrolysis and for SRFC applications.[36,60] The total area of PEC cells (*A*) required to achieve 1 kW and 20 kW can be calculated with the following equation:

$$A = \frac{P}{\Delta H^{\circ} \cdot j} \qquad 3.1$$

where *P* is the power and ΔH° is the redox potential difference between the two redox pairs.

An important indicator of the performance of photoelectrodes is the solar-to-chemical conversion efficiency (STCE), which can be calculated with the following equation:

$$STCE = \frac{j \cdot \Delta H^{\circ} \cdot t}{I} \qquad 3.2$$

where *t* is the amount of time with sunlight and I is the incident irradiation.

Regarding the stability of the semiconductor materials, α-Fe_2O_3 has been studied and proved to be very stable,[41] while $BiVO_4$ needs the deposition of protective layers and catalysts to improve its stability. Having this in mind it was assumed that the hematite semiconductors have an operation time of 10 years and the $BiVO_4$ have 5 years.

The electrolyte will be used as a thermal fluid, serving for thermal comfort of the implemented building. In this work it was considered that 100 m of tubes is enough to cover the building and additional 1 m needs to be added for each PEC cell installed.

3.4 Electrolytes

The photoelectrodes studied in this work are photoanodes and for that reason it was decided to maintain the same positive electrolyte, ferricyanide/ferrocyanide ($Fe(CN)_6^{3-}$/ $Fe(CN)_6^{4-}$) redox pairs in 1 M KOH, which is known to form good junctions with semiconductors. For the negative electrolyte, two different redox pairs were studied: one anthraquinone (9,10-anthraquinone-2,7-disulphonic acid) and one POM (SiW_{12}). The combination of ferrocyanide/AQDS (2,7) redox pairs has already been reported for SRFC systems based on hematite, presenting a concentration of 0.2 M and 0.1 M, respectively.[32] These concentrations will be used in the economic analysis for this combination of redox pairs. On the other hand, there are not any reports about the use of POMs in SRFC systems, but there are few reports about the use of POMs in RFBs. In these works, POMs are studied in small concentration, in the order of 10 mM.[23,52] Since these materials have very high energy densities and high solubility, the effects of the concentration will be studied in the economic viability of the application of these materials in a SRFC. The concentrations studied are 0.04 M/0.01 M and 0.4 M/0.1 M for the combination ferrocyanide/SiW_{12}. SiW_{12} can donate four electrons, while ferrocyanide can only donate one, the difference between the concentration of the two electrolytes makes it possible to use the same volume of electrolyte on the positive and negative side of the SRFC.

Table 3.2 presents the cost of aqueous electrolytes with different concentrations.

Table 3.2 – Cost of electrolytes.

Electrolyte	Concentration / M	Cost / €·L^{-1}
Ferrocyanide	0.04	9.0
	0.20	17.1
	0.40	27.2
AQDS	0.10	195.0
SiW_{12}	0.01	66.3
	0.10	646.6

The electrolyte is where the energy is stored. Thus, it is important to calculate the volume of electrolyte that the SRFC system needs, since that determines the amount of energy that can be converted into chemical energy. Utilizing Faraday's law and the power (*P*) of the system, the material flow of the active redox pair (*Q*) is calculated:[59]

$$Q = \frac{P}{n \cdot F \cdot U} \tag{3.3}$$

The amount of redox pairs (*N*) necessary in the positive and negative electrolyte can then be computed with the following equation:[59]

$$N = \frac{3600\ Q \cdot t_D}{DOD} \tag{3.4}$$

where t_D is the time of discharge in h and *DOD* is the depth of discharge, *i.e.* the difference between the maximum and minimum state of charge achieved ($DOD = SOC_{max} - SOC_{min}$). It was considered that the maximum SOC of the electrolyte will be 90 % and the minimum 40 %.

Knowing the amount of redox pairs required and the concentration of the electrolytes, the volume that will be needed is easily calculated. It was assumed that the tanks where the electrolytes are stored need to have one and a half times the volume of electrolyte stored.[59]

The energy efficiency of the electrolytes was considered to be 90 % and constant for all the combinations and concentrations.

3.5 Redox Flow Battery

The RFB part of the SRFC system is where the electrolytes discharging occurs. The vanadium redox flow batteries (VRFBs) were used as reference due to the extensive work performed until now. Minke *et al.*[59] made a techno economic assessment of large-area VRFBs and this analysis was adapted for the present work. Table 3.3 has the relevant prices in a RFB.

Table 3.3 – RFB componentes price.

Component	Price
Membrane	1 700 €·m^{-2}
Carbon Felt	100 €·m^{-2}
Graphite Plate[59]	200 €·m^{-2}
Current Collector[59]	3000 € per unit
Cell Frame and Gaskets[59]	200 € per unit
Stack Frame[59]	25 000 € per unit
Stack Assembly[59]	26 450 € per unit
Converter[59]	100 000 €·MW^{-1}
Cabling[59]	4 000 €·MW^{-1}
PCS (Process Control System)[59]	50 000 per system
Tanks[59]	300 €·m^{-3}
Pump[59]	64 €·h·m^{-3}
Assembly of the System	20 % of the investment
O&M	5 % of the investment

To implement this device in a household the output electrical potential must be 220 V, since this is the standard potential difference in household electrical sockets; this can be achieved by stacking various cells. An analysis of polarization curves of the two electrolyte combinations was made to select an operation point. Figure 3.2 shows a representation of the polarization curves of the studied redox pairs, highlighting the chosen operation points.

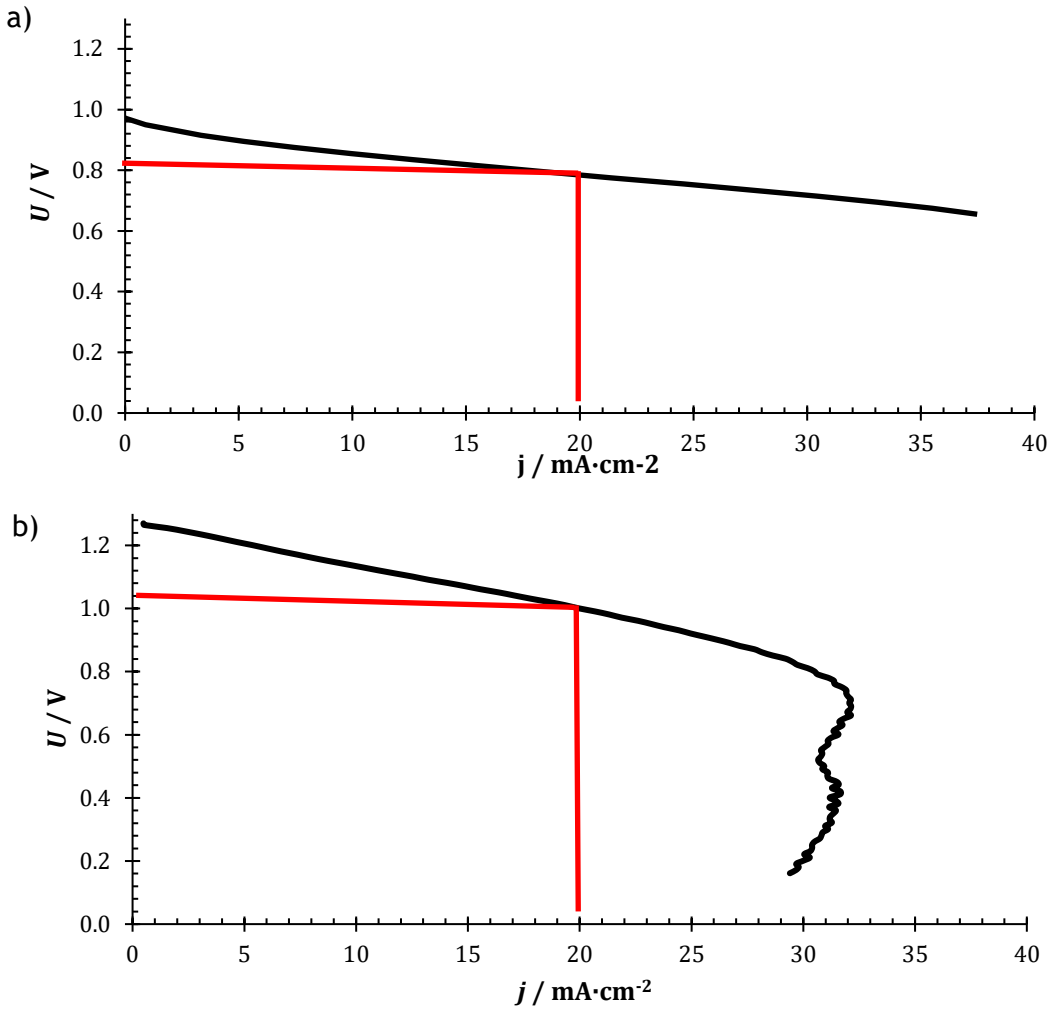

Figure 3.2 – Polarization curves of a) ferrocyanide/AQDS and b) ferrocyanide/SiW_{12} (preliminary results performed in collaboration with researchers at LEPABE).

The operation current density chosen was 20 mA·cm^{-2}, which results in a cell potential of 0.82 V for ferrocyanide/AQDS and 1.4 V for ferrocyanide/SiW_{12}.

The polarization curve for the combination ferrocyanide/SiW_{12} was done with small concentrations, which may not be a good representation of a polarization curve for a concentration 10 times bigger. To solve this problem, it was considered that the POM electrolyte with a bigger concentration has the same current density and potential as a Vanadium electrolyte. In the same work by Minke *et al.*,[59] they considered an operating current density of 100 mA·cm^{-2} and a potential of 1.244 V.

Considering these values for the operation of the RFB, the amount of cells in a stack and the number of stacks needed were calculated. Table 3.4 presents all the relevant data related to the RFB cost analysis.

Table 3.4 – Information about the cells and stacks of the RFBs.

	Ferrocyanide/ AQDS		Ferrocyanide/ SiW_{12} 0.01 M		Ferrocyanide/ SiW_{12} 0.1 M	
	1 kW	20 kW	1 kW	20 kW	1 kW	20 kW
Active Cell Area / m^2	0.025		0.025		0.025	
Operational Electrical Potential / V	0.82		1.04		1.244	
Operational Current Density / $kA \cdot m^{-2}$	0.2		0.2		100	
Number of Cells per Stack	269		212		177	
Number of Stacks	1	19	1	19	1	4

One scenario that was also be studied is the case of charging a RFB with PV panels, the so-called PV-assisted RFB. For this scenario it will be used a VRFB, because the costs associated with them are well known and their implementation is growing worldwide. Minke *et al.*[59] calculated the cost of a VRFB system by the power and energy that is desired in the system:

$$C_{system} = 1080\,P + 385\,E \qquad 3.5$$

where the cost of the system (C_{system}) is given in €.

3.6 Photovoltaic

At the moment, the low performances are the main limiting factor of SRFC systems for practical applications. By coupling PV panels, higher photopotentials can be reached. This scenario was considered to assess the viability of this solution. The use of PV panels will also be used in the more "practical" scenario, where they are connected to a VRFB.

Crystalline silicon (c-Si) PV panels are the most implemented type of PV systems. For that reason, they are the ones selected for this study. The website "Photovoltaic Geographical Information System" (https://re.jrc.ec.europa.eu/pvg_tools/en/tools.html) of the European Commission was used to estimate the power of PV panels required to produce the energy necessary. The power was estimated in representative points of each country, in the coordinates 39.324 º Lat, -7.637 º Lon and 55.942 º Lat, 9.299 º Lon for Portugal and Denmark, respectively. It was used the option for the software to optimize the slope and azimuth of the

panels, and it was considered 16 % of system loss. The price of silicon PV panels was reported to be 2.05 $\$\cdot Wp^{-1}$ in France, in 2015,[61] which converted to euros is *ca.* 1.88 $€\cdot Wp^{-1}$.

3.7 Solar Concentrating Devices

Solar irradiation concentration is a simple way to produce more energy using smaller areas. The implementation of concentrating technology with SRFC was also studied.

Dumortier *et al.*[62] reported the production of solar hydrogen using photoelectrochemical technologies. In this study, the price of different concentration technologies was averaged to a price of 201 $\$\cdot m^{-2}$, *ca.* 184 $€\cdot m^{-2}$. This may not be the best approach, however, since it is not possible to test which is the most suitable solar concentrator to pair with the SRFC technologies, this broader approach is a good approximation to the real cost.

The solar irradiation was quantified by the concentration ratio, *C*, which is the ratio between the area of the concentration device and the area of the PEC cell. It was considered an efficiency of 85 % for the solar concentration device.

3.8 Thermal Energy

An advantage of harnessing solar energy with SRFCs is that the electrolyte is in direct contact with the semiconductor, which is exposed to solar irradiation. This means that the electrolyte will heat up and the heat energy can be utilized *e.g.* for thermal comfort purposes.

The heating energy can be calculated by the solar irradiation that hits the PEC cell minus the losses in energy by convection and radiation. The coefficient of heat transfer by radiation between two parallel endless surfaces can be calculated using the following equation:

$$Q_R = \frac{A \cdot \sigma \cdot (T_1^4 - T_2^4)}{(1/\varepsilon_1) \cdot (1/\varepsilon_2) - 1} \qquad 3.6$$

where σ is the Stefan-Boltzmann constant, *T* is the temperature and ε is the emissivity. The polynomial can be written in the following way:

$$(T_1^4 - T_2^4) = (T_1^2 - T_2^2) \cdot (T_1^2 + T_2^2) = (T_1 - T_2) \cdot (T_1 + T_2) \cdot (T_1^2 + T_2^2) \qquad 3.7$$

Replacing this in Equation 3.6, comes:

$$Q_R = \frac{A \cdot \sigma \cdot (T_1 + T_2) \cdot (T_1^2 - T_2^2)}{(1/\varepsilon_1) \cdot (1/\varepsilon_2) - 1} \cdot (T_1 - T_2) \qquad 3.8$$

Losses by radiation are only made between the PEC cell glass and the air. Since air's emissivity is equal to 1, the coefficient of heat transfer by radiation ($h_{r,g-a}$) can be obtained:

$$h_{r,g-a} = \varepsilon_g \cdot \sigma \cdot (T_g + T_a) \cdot (T_g^2 + T_a^2) \qquad 3.9$$

where ε_g is glass' emissivity. And so, the global coefficient of heat transfer of the PEC cell is the sum of the coefficients of heat transfer by radiation and by convection ($h_{c,g-a}$).

$$U_L = h_{c,g-a} + h_{r,g-a} \quad 3.10$$

The energy transferred to the electrolyte (Q_u) can be calculated with Equation *3.11*.

$$Q_u = A_c \cdot \left[G \cdot (\tau \cdot \alpha) - U_L \cdot \left(T_g - T_a\right)\right] = \dot{m} \cdot c_P \cdot (T_{out} - T_{in}) \quad 3.11$$

where A_c is the area of the PEC cell, *G* is the total irradiation on a surface, τ and α are the transmittance and absorbance of glass, T_g and T_a are the temperatures of the glass and of the air, $\dot{m}$ is the mass flow of electrolyte, c_P is the thermal capacity of the electrolyte and T_{out} and T_{in} are the temperatures of the electrolyte in the inlet and in the outlet of the PEC cell.

Keeping in mind that the electrolyte is an aqueous solution, its properties were considered to be the properties of water, in particular heat capacity and density, 4186 $J \cdot kg^{-1} \cdot K^{-1}$ and 1000 $kg \cdot m^{-3}$. The other constants used in these calculations are presented in Table 3.5.

Table 3.5 – Relevant constants for the calculation of the thermal energy harnessed.

	Without solar concentration		**With solar concentration**	
	Portugal	**Denmark**	**Portugal**	**Denmark**
ε_g [63]	0.38			
T_g / K	303	295	423	415
T_a / K	291	283	291	283
$\tau \cdot \alpha$	0.016			
$\dot{m}$ / $m^3 \cdot h^{-1}$	0.4			
T_{in} / K	293			

3.9 Economic analysis

The economic analysis is made by comparing certain indicators, like payback time and levelized cost of energy (LCOE). The payback time is calculated by a balance between the investment and the money that is saved with the energy produced, during the lifetime of the SRFB. It shows how many years it takes to recuperate the money invested.

LCOE is the ratio between the total investment during the lifetime of the technology and the total energy produced during the same period of time. This value allows comparisons between different technologies, since it shows the price of energy produced by each technology.

4 Results and Discussion

This chapter presents the results of the economic analysis conducted for off-grid solar electrification using the SRFC technology. The assessment comprises the use of four different device designs: 1) a SRFC integrating a PEC cell and RFB; 2) a SRFC coupled with PV panels; 3) a SRFC operated under solar concentration; and 4) PV-assisted VRFB. The PV-assisted VRFB design is the only mature technology and will serve as reference. The aim of this work is to compare the influence of device design, materials combinations/choices, namely the two main components in a SRFC - photoelectrodes and redox pairs/electrolytes, operating conditions (*e.g.* using concentrated and non-concentrated irradiation), location and scalability, on the efficiency, price, manufacture, operation energy balance, and operating time of SRFCs. Figure 4.1 presents a schematic summary of the device and the component considerations/choices made in this work.

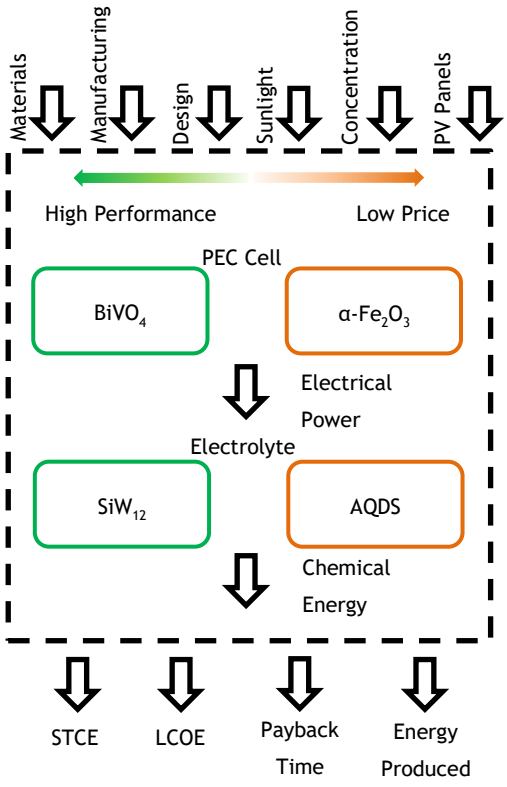

Figure 4.1 – Schematic summary of the inputs, outputs, materials and configurations studied.

A sensibility analysis was also made and the materials choice and device design that require technical improvements to turn the solar charging redox flow cells technology economically viable were discussed.

4.1 SRFC

The use of SRFCs holds great promises as compact, sustainable and cost-effective standalone energy systems for simultaneous conversion and storage of solar energy when compared with decoupled solar cells and batteries. Table 4.1 shows the variation of the three output metrics, such as the total energy produced during the lifetime (GWh), the levelized cost of energy (LCOE, €·kWh^{-1}) and the payback time (years), according to the different combinations under study: photoelectrodes ($BiVO_4$ and α-Fe_2O_3), redox pairs/electrolytes (0.2 M ferrocyanide/0.1 M AQDS 2,7; 0.04 M ferrocyanide/0.01 M SiW_{12}; 0.4 M ferrocyanide/0.1 M SiW_{12}), location (Portugal and Denmark) and scalability (power installations of 1 kW and 20 kW) and in Table A.1 is shown the investment of each component of the SRFC.

Table 4.1 – Total energy produced during lifetime, LCOE, payback time and number of PEC cells required for all the studied configurations of photoelectrode, redox pair/electrolyte, location and scalability, i.e. power installations.

Output metrics			**Energy produced / GWh**		**LCOE / €·kWh^{-1}**		**Payback time / years**		**Number of PEC cells**	
Scale			**1 kW**	**20 kW**	**1 kW**	**20 kW**	**1 kW**	**20 kW**	**1 kW**	**20 kW**
Denmark	**SiW_{12} – 0.1 M**	**$BiVO_4$**	1.7	32.4	0.89	0.74	-	-	13	252
		α-Fe_2O_3	8.8	174.5	0.25	0.21	17.0	13.8	70	1392
	SiW_{12} – 0.01 M	**$BiVO_4$**	1.7	32.4	0.96	0.91	-	-	13	252
		α-Fe_2O_3	8.8	174.5	0.27	0.22	19.3	14.9	70	1392
	AQDS – 0.1 M	**$BiVO_4$**	2.8	53.9	0.67	0.98	-	-	22	424
		α-Fe_2O_3	14.8	293.4	0.21	0.17	14.1	11.2	118	2346
Portugal	**SiW_{12} – 0.1 M**	**$BiVO_4$**	0.5	39.4	3.42	0.70	-	-	13	252
		α-Fe_2O_3	10.7	211.9	0.23	0.19	-	17.2	70	1392
	SiW_{12} – 0.01 M	**$BiVO_4$**	0.5	39.4	3.71	0.85	-	-	13	252
		α-Fe_2O_3	10.7	211.9	0.24	0.20	-	18.7	70	1392
	AQDS – 0.1 M	**$BiVO_4$**	3.4	65.4	0.60	0.57	-	-	22	424
		α-Fe_2O_3	17.9	356.3	0.18	0.18	17.0	16.8	118	2346

i) Photoelectrode

The four device indicators – performance, cost, sustainability, and degradation – must be considered when a photoelectrode is selected. In terms of efficiency, stability and abundance $BiVO_4$ and α-Fe_2O_3 photoelectrodes are the most promising metal-oxides studied up to date. Concerning the price of fabrication, $BiVO_4$ photoelectrodes are more expensive than α-Fe_2O_3 (2500 €·m^{-2} *vs* 1000 €·m^{-2}). However, nowadays $BiVO_4$ is capable of producing higher photocurrents (*ca.* 5 times higher than α-Fe_2O_3), which results in the installation of fewer PEC cells to produce the same power, thus leading to a lower final investment.

On the other hand, since it was considered that the electrical energy produced is equal for both photoelectrodes (Table 4.2), having fewer PEC cells reduces the thermal energy produced. The amount of global energy produced (electric and thermal) is then 5 times higher when the SRFC is equipped with PEC cells based on α-Fe_2O_3 photoelectrodes, as it can be seen in Table 4.1. Even though the investments are bigger using α-Fe_2O_3 photoelectrodes (Table 4.1), this material makes the SRFC technology a more profitable investment when the available area for technology application is not a disadvantage. It is important to refer that in this analysis it was not considered the cost of land needed for the installation, which could be a factor to benefit $BiVO_4$ over α-Fe_2O_3.

Table 4.2 – Energy produced in Portugal and Denmark in an installation with 1 kW and 20 kW.

Location	**Portugal**		**Denmark**	
Power / kW	1	20	1	20
Daytime / h	8.5		7	
E_{prod} **/ kWh**	8.5	170	7	140

ii) Electrolyte

The electrolyte used must be cheap, but also have a high energy density to store more energy with a smaller volume. However, having a lower cell potential difference between the redox couples, increases the area needed to produce a certain power, which increases the amount of thermal energy produced.

The SiW_{12} POM electrolyte is more expensive than AQDS, if the concentrations used are equal. When a concentration of 0.1 M is used, AQDS has a lower energy density than SiW_{12}, which causes them to have a similar overall investment. In this study, AQDS redox pair is the best choice for the electrolyte, since allows to increase the thermal energy produced.

iii) Location

In terms of energy produced, Portugal has the advantage over Denmark. However, Denmark is the place where the return of the investment is faster. This can be explained by the differences in the higher average solar irradiance (1700 $kWh \cdot m^{-2}$ in Portugal *vs* 1001 $kWh \cdot m^{-2}$ in Denmark) and the lower price of electricity (0.2150 $€ \cdot kWh^{-1}$ in Portugal *vs* 0.2984 $€ \cdot kWh^{-1}$ in Denmark).

Therefore, the LCOE of the technology is lower in Portugal, but the investment in this technology is much more profitable in Denmark.

iv) Scalability

The installation of SRFCs with 20 kW not only reduce the LCOE, but also the payback time of the investment. The profit made is highly increased from small to large scales, however this may be another case where the cost of land could be a decisive factor. Increasing the scale also increases the area that needs to be occupied to achieve the power desired.

Discussion

The use of standalone SRFCs proved to be economically viable in terms of thermal energy needs (energy for heating, cooling and hot water) when α-Fe_2O_3 and AQDS are used as photoanode and negative electrolyte, respectively. Even though using 0.1 M AQDS results in a bigger investment than using 0.1 M SiW_{12} electrolyte, its use increases the number of PEC cells that need to be installed.

Denmark is the preferred location in terms of money saved for electricity production. However, the production of energy in Portugal exceeds the energy produced in Denmark; this is why the LCOE is smaller in Portugal.

Scalability also influences the relation between investment and savings in energy. It was concluded that larger scales benefit the overall investment, *i.e.* the LCOE values are smaller, like the payback times. However, it is important to know how each component of the SRFC contributes to the overall investment. Figure 4.2 shows the fraction of cost of each component to the overall investment, considering the technology implementation in Denmark, with AQDS as redox pair/electrolyte and 1 kW scale.

For assembling the PEC cells (without considering photoelectrodes preparation and electrolytes), the investment obtained with α-Fe_2O_3 was 3 104 k€, while using $BiVO_4$ amounts to 1 860 k€. The investment in electrolyte and in the RFB is equal for both photoelectrode materials. The major difference between these two cases is the number of PEC cells that are required to be installed. Using α-Fe_2O_3, the installation needs to have 118 cells, whereas only 22 are needed using $BiVO_4$. These values explain the relative contribution of the PEC component

for each case. However, there is a difference of 12 GWh in the energy produced between them, as it is shown in Table 4.1.

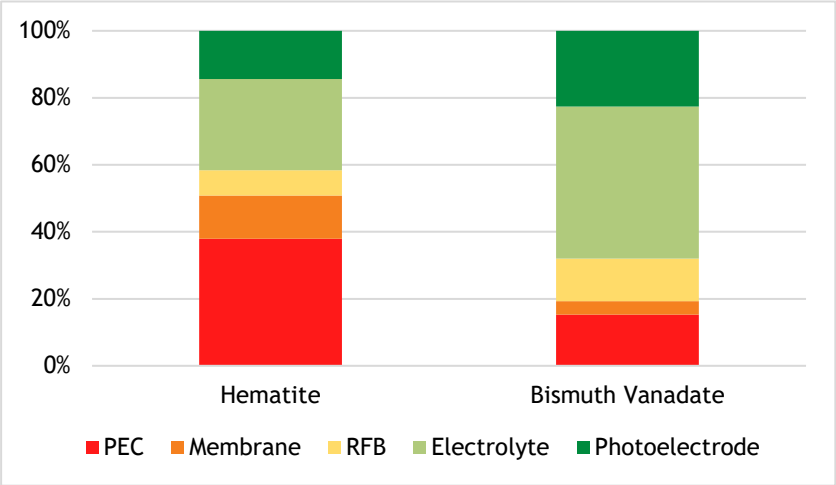

Figure 4.2 - Relative contributions to the overall investment in SRFCs, using hematite and bismuth vanadate as photoelectrodes.

Electrolyte has a great contribution to the overall investment in both scenarios. If POMs reach the price of AQDS, they would probably be the better choice to be implemented in this technology.

The scenarios previously presented are only possible in places where large terrain areas are available, however in the case of a house, the area available is limited, and so it is important to know the best configuration for this type of installation. Therefore, an installation using only one PEC cell with an active area of 2 m^2 was considered for the economic analysis. Herein, better performances for both semiconductors were considered: photocurrent densities of 4.0 $mA{\cdot}cm^{-2}$ and 6.5 $mA{\cdot}cm^{-2}$ for α-Fe_2O_3 and $BiVO_4$, which are the average of the highest values reported to date with these materials for PEC water splitting systems (these values were only considered in this scenario).[43,64] Table 4.3 shows the relevant results obtained for this economic analysis.

Table 4.3 – Energy produced (electric and thermal), investment, savings in energy, LCOE and STCE of an installation using a SRFC with one PEC cell.

Output metrics			Energy produced / GWh		Investment / k€	Savings / % of total investment	LCOE / €·kWh^{-1}	STCE / %
Type of energy			Electric	Thermal				
Denmark	SiW_{12} – 0.1 M	$BiVO_4$	7.35	6.2	185.4	5.20	1.40	18.3
		α-Fe_2O_3	4.52	6.2	170.0	5.17	1.32	11.3
	SiW_{12} – 0.01 M	$BiVO_4$	7.35	6.2	207.8	4.63	1.57	18.3
		α-Fe_2O_3	4.52	6.2	192.5	4.57	1.49	11.3
	AQDS – 0.1 M	$BiVO_4$	4.36	6.2	201.3	4.34	1.56	10.9
		α-Fe_2O_3	2.68	6.2	151.3	5.44	1.19	6.7
Portugal	SiW_{12} – 0.1 M	$BiVO_4$	8.92	7.6	200.2	4.21	1.25	13.1
		α-Fe_2O_3	5.49	7.6	184.9	4.16	1.18	8.1
	SiW_{12} – 0.01 M	$BiVO_4$	8.92	7.6	296.7	2.84	1.85	13.1
		α-Fe_2O_3	5.49	7.6	209.4	3.67	1.34	8.1
	AQDS – 0.1 M	$BiVO_4$	5.29	7.6	216.8	3.53	1.38	7.8
		α-Fe_2O_3	3.26	7.6	160.9	4.48	1.04	4.8

By using one PEC cell the production of thermal energy is equal for all the materials used (6.2 GWh in Denmark and 7.6 GWh in Portugal), the comparison in terms of electric energy produced is possible. Thus, the production of electric energy is 1.6 times higher with $BiVO_4$ photoelectrodes, however the cheaper photoelectrodes are still the better choice, *i.e.* α-Fe_2O_3. This can be concluded by the LCOE values, which are smaller using α-Fe_2O_3; the investments are too big compared to the money that is saved in the production of electric and thermal energies.

Regarding the electrolyte, using the SiW_{12} POM with a concentration of 0.1 M leads to more energy produced, since the cell potential difference between the redox couples is higher than with AQDS (1.11 *vs* 0.66). Which translates in a smaller investment in electrolyte using AQDS.

4.2 SRFC coupled with PV panels

In this scenario it was calculated the electrical energy produced by one PEC cell, and the rest of the energy was complemented by PV panels. Table 4.4 presents the SOC that was achieved by each combination of photoelectrode/electrolyte and their respective LCOE, for an installed power of 1 kW and 20 kW.

Table 4.4 – SOC achieved by one PEC cell using different combinations of photoelectrode and electrolyte and LCOE values for these configurations, for a power installation of 1 kW and 20 kW.

		SOC / %		LCOE / €·kWh^{-1}	
Electrolyte	**Photoelectrode**	**1 kW**	**20 kW**	**1 kW**	**20 kW**
AQDS	**α-Fe_2O_3**	0.85	0.04	6.71	18.78
	$BiVO_4$	4.72	0.24	6.73	18.79
SiW_{12}	**α-Fe_2O_3**	1.44	0.07	6.24	14.77
	$BiVO_4$	7.96	0.4	6.26	14.78

$BiVO_4$ harnesses more energy than α-Fe_2O_3, this lowers the investment that is required in PV panels. However, the difference of investment in PV does not cover the difference of investment in the two photoelectrodes. In a 20 year lifespan the investment in $BiVO_4$ photoanodes amounts to 19 k€, while the investment in α-Fe_2O_3 amounts to *ca.* 4 k€.

The electrolyte is another component that influences the amount of energy produced in the PEC cell. The POM redox pair allows a higher cell potential, which is translated in more energy produced. Besides that, the investment is also slightly smaller for the POM electrolyte.

With this configuration, the best-case scenario is to use a junction with α-Fe_2O_3 and 0.1 M SIW_{12}, in Denmark, for a 1 kW installation. Even so, the total investment amounts to 1 095 k€, and the savings in energy produced only cover 4.8 % of this investment. The LCOE is 6.24 €·kWh^{-1}.

Discussion

Coupling PV panels to SRFCs reduces the overall investment, but none of the studied combinations of photoelectrode, electrolyte, scale and location is profitable. Limiting the number of PEC cells to one, largely reduces the amount of thermal energy produced, and this is the main form of energy that is harnessed in PEC cells. Even with a big reduction, thermal energy is still 71 % of the total energy produced for an installation with 1 kW. For an installation with 20 kW it is only 11 % of the total energy produced.

Using only one PEC cell is not beneficial, however using PEC cells to achieve a higher SOC, may be. Using PEC cells to achieve 50 % of the SOC, while also producing thermal energy, and having the rest of the energy produced by PV panels, reduces the total investment. This might be a solution that is more profitable than only using SRFC, but it was not studied in this work.

The electrolyte is the biggest investment in this scenario, *ca.* 70 % of the total investment. Figure 4.3 presents the contribution of the different parts of the SRFC and of PV to the total investment, using hematite and bismuth vanadate as photoelectrodes and SiW_{12} redox pair in the negative electrolyte with a concentration of 0.1 M, for an installation with 1 kW, in Denmark.

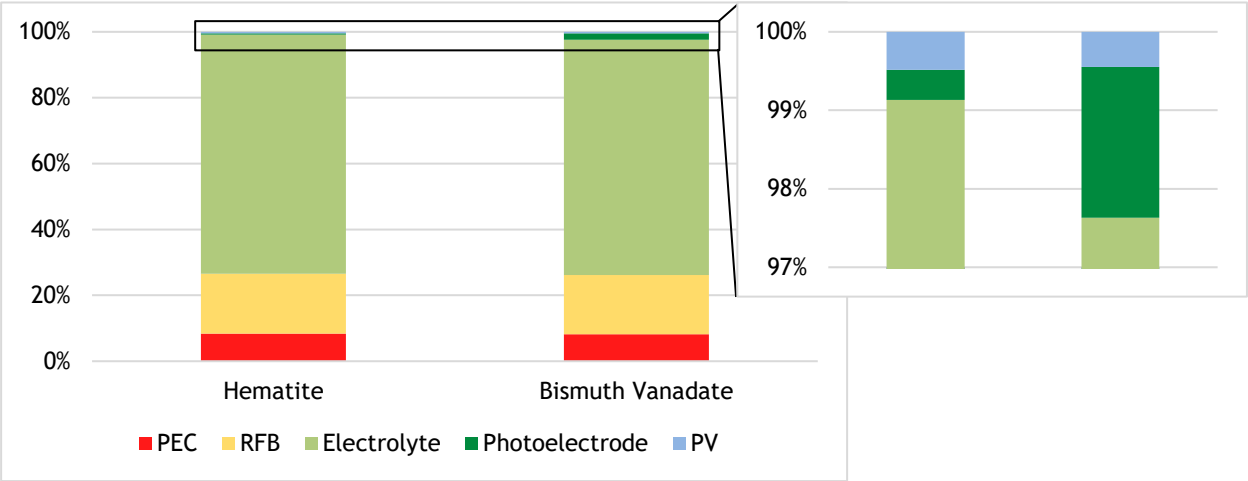

Figure 4.3 - Relative contributions to the overall investment in SRFCs and PV panels, using hematite and bismuth vanadate as photoelectrodes.

The total investment using hematite is 1 097 k€ and using bismuth vanadate is 1 114 k€. The biggest contributor to this investment is the electrolyte. It is foreseeable that the cost of this component will decrease, because POMs have been the focus of various studies regarding their application in RFBs. If the cost of electrolyte receives a considerable decrease, this configuration will be much closer to becoming a possible solution for the implementation of SRFBs.

4.3 Solar Concentration

The main problem of the SRFC system is the large number of PEC cells needed to achieve power in the order of the kW scale. Coupling this technology with PV panels can reduce the number of PEC cells required, but that also reduces the amount of thermal energy produced. Using solar concentration may solve these problems. By concentrating solar radiation, the number of PEC cells installed is reduced, leading to a decrease in the overall investment, and it also increases the production of thermal energy.

For the implementation of solar concentration, it was only considered the use of 0.1 M SiW_{12} as electrolyte, since it is the electrolyte that has a smaller investment. The concentration ratios required to achieve 1 kW and 20 kW are presented in Table 4.5, as well as the number of PEC cells needed and the photocurrent that is achieved with these concentration ratios. The values presented correspond to the lowest investments.

Table 4.5 - Concentration ratio, number of PEC cells, current density and LCOE in an installation with 1 kW and 20 KW.

Output metrics			***C***		**Number of PEC cells**		***j* / mA·cm^{-2}**		**LCOE / €·kWh^{-1}**	
Country			**Portugal**	**Denmark**	**Portugal**	**Denmark**	**Portugal**	**Denmark**	**Portugal**	**Denmark**
1 kW	**SiW_{12}**	**$BiVO_4$**	15		1		45.9		0.72	0.76
		α-Fe_2O_3	82		1		45.3		0.73	0.77
20 kW	**SiW_{12}**	**$BiVO_4$**	81.5		4		249.4		6.91	7.00
		α-Fe_2O_3	452		4		249.7		2.59	2.64

Contrarily, to complementing SRFBs with PV panels, using solar concentration benefits from the use of $BiVO_4$, since this material reduces the investment in concentration devices, because of its better performance. The best scenario with this configuration is its implementation in Denmark, which leads to a total investment of 1 285 k€, saving a total of 433 k€ in electric and thermal energy and a LCOE of 0.77 €·kWh^{-1}.

Implementing this technology may have some disadvantages, like the reduction in lifetime of some components of the PEC cell or the creation of gas bubbles in the electrolyte, if it reaches high temperatures. These problems were not considered in this work but must be kept in mind in the development of this configuration.

Discussion

Using solar concentration showed better results than using PV panels coupled with SRFCs, however this scenario is not profitable. Despite the number of PEC cells required being reduced

and the amount of thermal energy produced per PEC cell increasing, the thermal energy produced is still not enough to cover the total investment made. Figure 4.4 presents the contribution of each component of this scenario to the overall investment.

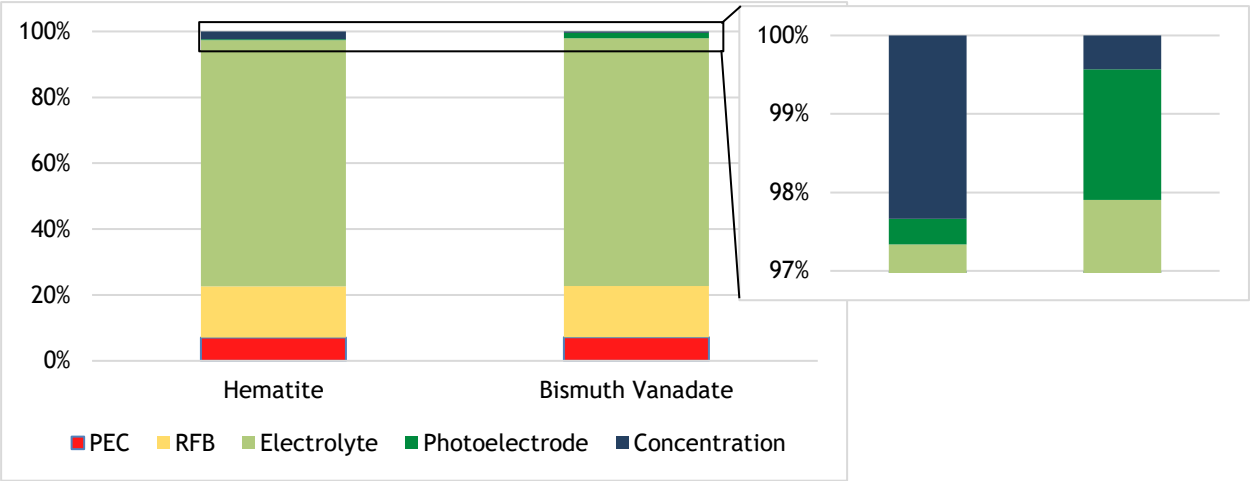

Figure 4.4 - Relative contributions to the overall investment in SRFC and solar concentration devices, using hematite and bismuth vanadate as photoelectrodes.

The investment in electrolyte comprises the biggest of the total investment. Like it was said previously, a decrease in the cost of POM electrolytes may cause a great difference in the economic balance of this technology.

The total investment using $BiVO_4$ is smaller than using α-Fe_2O_3 (1 285 k€ vs 1 293 k€). This difference is justified by the higher photocurrent of bismuth, which leads to a smaller investment in the concentration device, covering the difference between the investment in the two semiconductors.

4.4 VRFB coupled with PV panels

PV panels and VRFBs are more mature technologies and have been commercialized for some years, which makes this scenario the only one profitable that was studied. The investment made in the PV-assisted VRFB technology only amounts to 8 154 € to produce and store 4 kWh per day, in Portugal. This value is much smaller than in the scenarios discussed previously.

Table 4.6 presents payback times and LCOE for the different scenarios that use PV panels coupled with a VRFB.

Table 4.6 – Payback time and LCOE for different scenarios using PV-assisted VRFB technology.

Country	Portugal		Denmark	
Scale (kW)	1	20	1	20
Payback time (years)	12.2		12.0	
LCOE (€·kWh^{-1})	0.13		0.18	

The energy produced and stored by these technologies is cheaper than the energy bought to the grid and the savings largely outweigh the investment made. This is the best option, even though the amount of energy produced is much smaller than in the scenarios using SRFCs due to the decrease in thermal energy production.

4.5 Sensibility Analysis

The sensibility analysis gives a better understanding of how the investment can change if some modifications are made to the prices or to the amount of energy produced. The analysis was made to the best scenario and to one of the worst scenarios using standalone SRFCs, to a scenario using PV panels coupled to SRFCs and to the scenario using SRFCs with solar concentration devices.

4.5.1 SRFC

The best scenario presented in this work that uses SRFCs based on hematite and AQDS, installed in Denmark with a scale of 20 kW. Some changes were made to the assumptions described earlier to study the effect of them on the investment. Table 4.7 presents a summary of the most important values from this analysis.

Table 4.7 – Sensibility analysis of the scenario using hematite and AQDS, in Denmark, on a 20 kW installation.

Changes made	**-**	**Lifetime of photoelectrode of 1 year**	**Lifetime of photoelectrode of 1 year + 50 % increase in the total investment**	**45 % reduction in thermal energy produced**	**25 % increase in thermal energy produced**
Energy produced / GWh	293.4	293.4	293.4	161.9	366.6
LCOE / €·kWh^{-1}	0.17	0.18	0.29	0.30	0.13
Payback time / years	11.2	11.6	19.5	-	9.0

The chemical stability of the photoelectrode in water-based electrolytes is one of the major drawbacks in a PEC cell. Most of the photoelectrodes start to degrade after some hours or even minutes of operating conditions. The photoelectrodes are deposited in very thin layers, and most of them starts to deteriorate extremely fast. $BiVO_4$ and α-Fe_2O_3 are the only two photoelectrodes reporting a stable behavior of 1000 h. However, considering a lifetime of one year did not present a problem to the overall investment, *i.e.* the LCOE and payback time only showed a slight increase.

The economic assessment uses realistic costs for the different components, however the considerations can vary. If the photoelectrode has a one-year lifetime, the worst-case scenario, and a 50 % increase in the total investment, the LCOE and payback time increased to 0.29 €·kWh^{-1} and 19.5 years, respectively. However, this proves that this configuration's investment can have a substantial increase and be economically viable.

The amount of thermal energy produced is one of the most important variables in this study. This value can suffer oscillations and is a factor that was never studied in SRFCs. This investment becomes unprofitable if the thermal energy produced is 45 %, or less, of the expected value. On the other hand, this value can also be bigger than expected, and it only needs to increase by 25 % for this technology to reach a LCOE equal to the one presented by the combination of PV panels and VRFB.

On the other hand, one of the worst scenarios for SRFC applications is the use of $BiVO_4$ and SiW_{12}, in Portugal, with an installation of 1 kW. So, it is interesting to understand what is needed to make this configuration a profitable investment. The simpler way to improve this investment is by reducing it; however, this reduction would have to be to 6 % of the initial investment, which is a very improbable scenario. Having this in mind and assuming a lifetime of 10 years for $BiVO_4$, it is also necessary to reduce the investment to 6 % of its initial value, to make the technology profitable.

Lastly, it was considered an increase in thermal energy produced. Assuming an investment equal to the base scenario, the thermal energy produced would have to increase 19 times to make the investment viable.

4.5.2 SRFC Coupled with PV Panels

The best materials to be used in a SRFC coupled with PV panels are hematite and SiW_{12}, because they are cheaper than the others under study. Using these materials for installing 1 kW SRFC in Denmark is the best option for this scenario.

As was seen before, the major drawback with this configuration is the reduction in thermal energy produced. To turn this into a profitable solution, the thermal energy produced would

have to be 30 times more efficient than the energy that is expected to be harnessed. A value very unlikely to achieved using only one PEC cell.

The prices of the SRFC technology will probably decrease over time, however, to make this scenario viable, the investment in the SRFC would have to decrease to 4 % of its initial value.

4.5.3 Solar Concentration

Solar concentration devices reduce the number of PEC cells required at a SRFC system, while also increase the amount of thermal energy that is harnessed by each PEC cell. This is a good addition to SRFCs, but the global energy produced is not enough to cover the investment made.

This configuration needs to produce 3 times more energy to become a profitable investment. This is probably achievable, however SRFCs require special attention concerning the stability behavior of the photoelectrode/electrolyte junction, since it can degrade if it reaches very high temperatures. The investment needs to be 37 % of its original value to become a viable option.

5 Conclusion

The present thesis proposes the use of solar redox flow cells (SRFCs) for efficient and stable PEC solar energy conversion and electrochemical energy storage, easily convertible into electricity at a RFB. The SRFC technology has the potential to cover the daily cycle energy needs and provide cogeneration of thermal energy, which makes it especially suitable for the residential and office buildings.

It is challenging to predict when the SRFCs will be ready to compete with the electrically coupled solar cell and RFB storage systems. There are still too many challenges to be addressed before practical application could be launched into the market. This work aims at performing the first cost analysis for SRFCs using four indicators: performance, cost, device manufacture and operation energy demand. Different design configurations – SRFC integrating a PEC cell and RFB; SRFC coupled with PV panels; SRFC operated under solar concentration; and PV-assisted VRFB – and materials – photoelectrodes of hematite and bismuth vanadate; combination of redox pairs of ferrocyanide / AQDS 2,7 and ferrocyanide / SiW_{12}, are addressed in this study. The redox pairs were chosen for their availability, performance and knowledge at LEPABE.

It was concluded that larger harvest areas make the investment in SRFCs profitable, even though the costs are also higher. For this case, the electric energy was maintained constant and the number of PEC cells was varied, considering a PEC panel of 2 m^2. It was observed that there is no need to fabricate more energy efficient semiconductors, *i.e.* the combination of stable α-Fe_2O_3 photoelectrodes displaying low power conversion efficiencies and ferrocyanide / AQDS 2,7 redox pairs/ electrolytes with low cell potential proved to be the most effective option, allowing to produce more thermal energy. However, comparing the same number of PEC cells, the best options are the cheaper ones, α-Fe_2O_3 and ferrocyanide/SiW_{12} with a concentration of 0.1 M. Concerning the scalability factor, installations producing more power (20 kW *vs* 1 kW) are more profitable, as expected.

For practical applications, when the exposed free area is a limiting parameter, *i.e.* for minimum land uses such as at residential buildings, there is a close relation between the design for maximized performance over operational time and for maximum energy output. In this case, only one PEC cell of 2 m^2 was considered and the thermal energy was maintained constant. Thus, the combination of $BiVO_4$ photoelectrode and ferrocyanide/SiW_{12} redox pairs allowed to produce the highest electric power, despite the higher investment.

Applying solar concentration devices showed cost and efficiency advantages compared to non-concentrated case; its application is also competitive and sustainable with minimum land use scenarios. This arrangement reduces the amount of PEC cells needed and increases the thermal energy produced by each cell, making it an option closer to be a viable investment. Moreover,

the use of high concentration factors can lead to increase significantly the electric energy, while allowing the use of fewer number of PEC cells; however, this study was out of the objectives of this work. On the other hand, when PV panels are coupled to SRFCs, using the configuration considered in this study, the technology became unprofitable. However, the PEC-PV tandem configuration needs to be studied, where the PV cell will provide an extra bias potential for increasing the generated photovoltage and the state-of-charge of the SRFC, which should originate higher energy efficiencies (electric and thermal).

In conclusion, the best scenario studied for SRFCs was based on the use of α-Fe_2O_3 as photoelectrode and ferrocyanide and AQDS redox pairs in the electrolyte, located in Denmark, and with a 20 kW installation. This scenario requires 2346 PEC cells to produce 293.4 GWh in 20 years (applicable for a neighborhood), has a LCOE of 0.17 €·kWh^{-1} and a payback time of 11.2 years, which are values close to an actual investment in PV panels and VRFB to produce the same power. The sensitivity analysis proved that this scenario can suffer changes from the original assumptions and continue to be viable. SRFCs made of 2 m^2 PEC cells are still a dream for this technology with no more than seven years of extensive research. However, this economic analysis can provide crucial guidelines for the assessment of SRFC designs, materials choices and operating conditions for a scalable and competitive solar off-grid electrification for the future. As future work, different types of materials under different design configurations will be studied, covering an exhaustive range of low-cost and high-performance solutions between photoelectrode and redox pairs/electrolytes. The integrated-PEC configuration will be studied for SRFC, which could be able to produce > 20 % solar-to-chemical efficiency (higher than the values assumed in this work). This configuration considers the thermally integration of PV modules in a cell electrolyser equipped with an alkaline membrane-electrode assembly (MEA).

6 Assessment of the work done

6.1 Objectives Achieved

Due to the pandemic outbreak, this thesis aimed at performing the first economic analysis for the SRFC technology. It was proposed the use of multi-objective studies to account for efficiency, price, manufacture and operation energy balance to provide guidelines for overall device design, material choices (varying fabrication costs and performances), and operating conditions (*e.g.* using concentrated irradiation), at different locations and scales. It was also compared with more mature technologies, PV-assisted RFBs. These objectives were successfully completed and the findings presented support the decision process for a practical approach.

6.2 Other Work Carried Out

The first goal of this work plan was the development and optimization of a highly efficient and stable SRFC based on the combination of stable metal-oxide photoelectrodes (hematite and bismuth vanadate) and POM redox pairs/electrolytes. Since hematite materials are well-studied at LEPABE, this thesis had two main objectives: i) the synthesis of bismuth vanadate; and ii) optimization of a suitable POM redox pair/photoelectrode combination. An extensive state of the art was performed on bismuth vanadate photoelectrodes for PEC water splitting and SRFC applications and their production by spray pyrolysis was initialized; to acquire know-how about this experimental setup hematite photoelectrodes were also prepared. Assembling of PEC/SRFC devices and their photoelectrochemical performance tests were also performed.

6.3 Final Assessment

The work developed in this thesis provides crucial information for future application of SRFCs. To date, there are no reports concerning the economic assessment of SRFC technologies. The findings presented here show that device design/size considerations, materials choice, operating conditions and location play a key role for achieving the four performance metrics needed for competitive and scalable technology: efficiency, price, sustainability, and stability. This study is a first attempt to contribute on the optimization of technical, economic, sustainability, and operating time constraints to support the future decision-making process for viable applications.

Renewable energies are being more implemented than ever, so developing new and more efficient ways to harness these sources of energy has never been so relevant. This work gave me insights not only on the laboratorial side of the research that goes into these technologies, but also on the economic side, that needs to be kept in mind in all projects.

7 References

1. Borduas N, Donahue NM. The Natural Atmosphere. In: Green Chemistry: An Inclusive Approach. Elsevier Inc.; 2018. p. 131–50.
2. Kirk-Davidoff D. The Greenhouse Effect, Aerosols, and Climate Change. In: Green Chemistry: An Inclusive Approach. Elsevier Inc.; 2018. p. 211–34.
3. NOAA National Centers for Environmental information. Climate at a Glance: Global Time Series [Internet]. 2020 [cited 2020 Apr 20]. Available from: https://www.ncdc.noaa.gov/cag/
4. Dlugokencky E, Tans P. NOAA/ESRL [Internet]. [cited 2020 Apr 20]. Available from: https://www.esrl.noaa.gov/gmd/ccgg/trends/
5. IRENA. Statistics Time Series [Internet]. [cited 2020 Mar 20]. Available from: https://www.irena.org/Statistics/
6. APREN. Renewable electricity in Portugal: Yearbook. 2019.
7. Krol R van de., Grätzel M. Photoelectrochemical hydrogen production. Vol. 102. Springer; 2012.
8. Jäger-Waldau A. Costs and Economics of Electricity from Residential PV Systems in Europe [Internet]. 2016 [cited 2020 Jul 3]. Available from: http://www.europeanenergyinnovation.eu/Articles/Winter-2016/Costs-and-Economics-of-Electricity-from-Residential-PV-Systems-in-Europe
9. van de Krol R, Parkinson BA. Perspectives on the photoelectrochemical storage of solar energy. MRS Energy Sustain. 2017;4:E13.
10. Schreier M, Luo J, Gao P, Moehl T, Mayer MT, Grätzel M. Covalent Immobilization of a Molecular Catalyst on Cu2O Photocathodes for CO2 Reduction. J Am Chem Soc. 2016 Feb 17;138(6):1938–46.
11. Solargis. Solar resource maps [Internet]. [cited 2020 Mar 17]. Available from: https://solargis.com/maps-and-gis-data/
12. Shigematsu T. Redox Flow Battery for Energy Storage. SEI Tech Rev. 2011 Oct;73:4–13.
13. Sum E, Skyllas-Kazacos M. A study of the V(II)/V(III) redox couple for redox flow cell applications. J Power Sources. 1985 Jun 1;15(2–3):179–90.
14. Materials Roadmap Enabling Low Carbon Energy Technologies. Brussels; 2011.
15. Cao L, Skyllas-Kazacos M, Wang D-W. Solar Redox Flow Batteries: Mechanism, Design, and Measurement. Adv Sustain Syst. 2018 Aug 1;2(8–9):1800031.
16. Bentien A, Mendes A, Andrade L. A solar rechargeable redox flow cell. WIPO; WO2015120858A1, 2015.
17. Directive (EU) 2018/844 of the European Parliament and of the Council of 30 May 2018

amending Directive 2010/31/EU on the energy performance of buildings and Directive 2012/27/EU on energy efficiency. L 156, 2018/844 Official Journal of the European Union; Jun 19, 2018 p. 75–91.

18. Li Q, Zhang L, Dai J, Tang H, Li Q, Xue H, et al. Polyoxometalate-based materials for advanced electrochemical energy conversion and storage. Chem Eng J. 2018 Nov 1;351:441–61.
19. Alotto P, Guarnieri M, Moro F. Redox flow batteries for the storage of renewable energy: A review. Renew Sustain Energy Rev. 2014;29:325–35.
20. Dias P, Azevedo J, Lopes T, Mendes A. Solar redox flow cells: a new frontier on solar energy storage. In: Proceedings of nanoGe Fall Meeting19. Berlin, Germany; 2019.
21. Nozik AJ. Photoelectrochemistry: Applications to Solar Energy Conversion. Annu Rev Phys Chem. 1978 Oct 28;29(1):189–222.
22. Dias P, Mendes A. Hydrogen Production from Photoelectrochemical Water Splitting. In: Encyclopedia of Sustainability Science and Technology. Springer New York; 2018. p. 1–52.
23. Friedl J, Holland-Cunz M V., Cording F, Pfanschilling FL, Wills C, McFarlane W, et al. Asymmetric polyoxometalate electrolytes for advanced redox flow batteries. Energy Environ Sci. 2018 Oct 1;11(10):3010–8.
24. Hodes G, Manassen J, Cahen D. Photoelectrochemical energy conversion and storage using polycrystalline chalcogenide electrodes. Nature. 1976 Jun 3;261(5559):403–4.
25. Liu P, Cao Y, Li G-R, Gao X-P, Ai X-P, Yang H-X. A Solar Rechargeable Flow Battery Based on Photoregeneration of Two Soluble Redox Couples. ChemSusChem. 2013 May 1;6(5):802–6.
26. Li W, Fu HC, Zhao Y, He JH, Jin S. 14.1% Efficient Monolithically Integrated Solar Flow Battery. Chem. 2018 Nov 8;4(11):2644–57.
27. Bae D, Faasse GM, Kanellos G, Smith WA. Unravelling the practical solar charging performance limits of redox flow batteries based on a single photon device system. Sustain Energy Fuels. 2019 Aug 20;3(9):2399–408.
28. Wedege K, Bae D, Smith WA, Mendes A, Bentien A. Solar Redox Flow Batteries with Organic Redox Couples in Aqueous Electrolytes: A Minireview. J Phys Chem C. 2018 Nov 15;122(45):25729–40.
29. Rothschild A, Dotan H. Beating the Efficiency of Photovoltaics-Powered Electrolysis with Tandem Cell Photoelectrolysis. ACS Energy Lett. 2017 Jan 13;2(1):45–51.
30. Azevedo J, Seipp T, Burfeind J, Sousa C, Bentien A, Araújo JP, et al. Unbiased solar energy storage: Photoelectrochemical redox flow battery. Nano Energy. 2016 Apr 1;22:396–405.
31. Liao S, Zong X, Seger B, Pedersen T, Yao T, Ding C, et al. Integrating a dual-silicon

photoelectrochemical cell into a redox flow battery for unassisted photocharging. Nat Commun. 2016 May 4;7(1):1–8.

32. Wedege K, Azevedo J, Khataee A, Bentien A, Mendes A. Direct Solar Charging of an Organic-Inorganic, Stable, and Aqueous Alkaline Redox Flow Battery with a Hematite Photoanode. Angew Chemie Int Ed. 2016 Jun 13;55(25):7142–7.
33. Cheng Q, Fan W, He Y, Ma P, Vanka S, Fan S, et al. Photorechargeable High Voltage Redox Battery Enabled by Ta3N5 and GaN/Si Dual-Photoelectrode. Adv Mater. 2017 Jul 12;29(26):1700312.
34. McKone JR, DiSalvo FJ, Abruña HD. Solar energy conversion, storage, and release using an integrated solar-driven redox flow battery. J Mater Chem A. 2017 Mar 14;5(11):5362–72.
35. Wedege K, Bae D, Dražević E, Mendes A, Vesborg PCK, Bentien A. Unbiased, complete solar charging of a neutral flow battery by a single Si photocathode. RSC Adv. 2018 Feb 6;8(12):6331–40.
36. Zhou Y, Zhang S, Ding Y, Zhang L, Zhang C, Zhang X, et al. Efficient Solar Energy Harvesting and Storage through a Robust Photocatalyst Driving Reversible Redox Reactions. Adv Mater. 2018 Aug 2;30(31):1802294.
37. Khataee A, Azevedo J, Dias P, Ivanou D, Dražević E, Bentien A, et al. Integrated design of hematite and dye-sensitized solar cell for unbiased solar charging of an organic-inorganic redox flow battery. Nano Energy. 2019 Aug 1;62:832–43.
38. Li W, Kerr E, Goulet M, Fu H, Zhao Y, Yang Y, et al. A Long Lifetime Aqueous Organic Solar Flow Battery. Adv Energy Mater. 2019 Aug 8;9(31):1900918.
39. Kim JH, Lee JS. Elaborately Modified BiVO4 Photoanodes for Solar Water Splitting. Adv Mater. 2019 May 21;31(20):1806938.
40. Dias P, Andrade L, Mendes A. Hematite-based photoelectrode for solar water splitting with very high photovoltage. Nano Energy. 2017 Aug 1;38:218–31.
41. Dias P, Vilanova A, Lopes T, Andrade L, Mendes A. Extremely stable bare hematite photoanode for solar water splitting. Nano Energy. 2016 May 1;23:70–9.
42. Pihosh Y, Turkevych I, Mawatari K, Uemura J, Kazoe Y, Kosar S, et al. Photocatalytic generation of hydrogen by core-shell WO3/BiVO4 nanorods with ultimate water splitting efficiency. Sci Rep. 2015 Jun 8;5(1):1–10.
43. Kim JH, Kaneko H, Minegishi T, Kubota J, Domen K, Lee JS. Overall Photoelectrochemical Water Splitting using Tandem Cell under Simulated Sunlight. ChemSusChem. 2016 Jan 8;9(1):61–6.
44. Tolod K, Hernández S, Russo N. Recent Advances in the BiVO4 Photocatalyst for Sun-Driven Water Oxidation: Top-Performing Photoanodes and Scale-Up Challenges. Catalysts. 2017 Jan 1;7(12):13.

45. Kuang Y, Jia Q, Ma G, Hisatomi T, Minegishi T, Nishiyama H, et al. Ultrastable low-bias water splitting photoanodes via photocorrosion inhibition and in situ catalyst regeneration. Nat Energy. 2017 Jan 11;2(1):1–9.
46. Gong K, Fang Q, Gu S, Li SFY, Yan Y. Nonaqueous redox-flow batteries: Organic solvents, supporting electrolytes, and redox pairs. Energy Environ Sci. 2015 Dec 1;8(12):3515–30.
47. Winsberg J, Hagemann T, Janoschka T, Hager MD, Schubert US. Redox-Flow Batteries: From Metals to Organic Redox-Active Materials. Angew Chemie - Int Ed. 2017;56(3):686–711.
48. Chen H, Cong G, Lu YC. Recent progress in organic redox flow batteries: Active materials, electrolytes and membranes. J Energy Chem. 2018 Sep 1;27(5):1304–25.
49. Er S, Suh C, Marshak MP, Aspuru-Guzik A. Computational design of molecules for an all-quinone redox flow battery. Chem Sci. 2015 Feb 1;6(2):885–93.
50. Huskinson B, Marshak MP, Suh C, Er S, Gerhardt MR, Galvin CJ, et al. A metal-free organic-inorganic aqueous flow battery. Nature. 2014 Jan 8;505(7482):195–8.
51. Lin K, Chen Q, Gerhardt MR, Tong L, Kim SB, Eisenach L, et al. Alkaline quinone flow battery. Science (80-). 2015 Sep 25;349(6255):1529–32.
52. Friedl J, Pfanschilling FL, Holland-Cunz M V, Fleck R, Schricker B, Wolfschmidt H, et al. A polyoxometalate redox flow battery: functionality and upscale. Clean Energy. 2019 Dec 6;3(4):278–87.
53. Pratt HD, Hudak NS, Fang X, Anderson TM. A polyoxometalate flow battery. J Power Sources. 2013 Aug 15;236:259–64.
54. Chen JJ, Symes MD, Cronin L. Highly reduced and protonated aqueous solutions of [P2W18O62]6− for on-demand hydrogen generation and energy storage. Nat Chem. 2018 Oct 1;10(10):1042–7.
55. Feng T, Wang H, Liu Y, Zhang J, Xiang Y, Lu S. A redox flow battery with high capacity retention using 12-phosphotungstic acid/iodine mixed solution as electrolytes. J Power Sources. 2019 Oct 1;436:226831.
56. Skalik L, Skalikova I. Long-term Global Radiation Measurements in Denmark and Sweden. IOP Conf Ser Mater Sci Eng. 2019;471:102004.
57. Cavaco A, Silva H, Canhoto P, Neves S, Neto J, Pereira MC. Annual Average Value of Solar Radiation and its Variability in Portugal. Vol. 1, Abstract Book | Livro de Resumos. 2016.
58. PORDATA - Preços da electricidade para utilizadores domésticos e industriais (Euro/ECU) [Internet]. 2020 [cited 2020 Jul 5]. Available from: https://www.pordata.pt/Europa/Preços+da+electricidade+para+utilizadores+domésticos+e+industriais+(Euro+ECU)-1477
59. Minke C, Kunz U, Turek T. Techno-economic assessment of novel vanadium redox flow batteries with large-area cells. J Power Sources. 2017 Jun;361:105–14.

60. Wedege K, Azevedo J, Khataee A, Bentien A, Mendes A. Direct Solar Charging of an Organic–Inorganic, Stable, and Aqueous Alkaline Redox Flow Battery with a Hematite Photoanode. Angew Chemie - Int Ed. 2016;55(25):7142–7.
61. Yu HJJ. A prospective economic assessment of residential PV self-consumption with batteries and its systemic effects: The French case in 2030. Energy Policy. 2018 Feb 1;113:673–87.
62. Dumortier M, Tembhurne S, Haussener S. Holistic design guidelines for solar hydrogen production by photo-electrochemical routes. Energy Environ Sci. 2015 Dec 1;8(12):3614–28.
63. Yang JK, Liang B, Zhao MJ, Gao Y, Zhang FC, Zhao HL. Reference of Temperature and Time during tempering process for non-stoichiometric FTO films. Sci Rep. 2015 Oct 14;5(1):1–6.
64. Gurudayal, John RA, Boix PP, Yi C, Shi C, Scott MC, et al. Atomically Altered Hematite for Highly Efficient Perovskite Tandem Water-Splitting Devices. ChemSusChem. 2017;10(11):2449–56.

Appendices A

Table A.1 – Investment in PEC cells, photoelectrodes, electrolyte and RFBs.

Component			PEC cells / k€		RFB / k€		Photoelectrode / k€		Electrolyte / k€	
Scale			1 kW	20 kW	1 kW	20 kW	1 kW	20 kW	1 kW	20 kW
Denmark	SiW_{12} – 0.1 M	$BiVO_4$	244	3 279	200	825	62	1 206	796	15 912
		α-Fe_2O_3	968	17 758			132	2 633		
	SiW_{12} – 0.01 M	$BiVO_4$	244	3 279	225	4 278	62	1 206	889	17 779
		α-Fe_2O_3	968	17 758			132	2 633		
	AQDS – 0.1 M	$BiVO_4$	358	5 463	236	4 442	105	2 028	844	16 887
		α-Fe_2O_3	1 578	29 874			223	4 437		
Portugal	SiW_{12} – 0.1 M	$BiVO_4$	244	3 279	201	833	62	1 206	966	19 322
		α-Fe_2O_3	968	17 758			132	2 633		
	SiW_{12} – 0.01 M	$BiVO_4$	244	3 279	228	4 352	62	1 206	1 079	21 589
		α-Fe_2O_3	968	17 758			132	2 633		
	AQDS – 0.1 M	$BiVO_4$	358	5 463	235	4 467	105	2 028	1 025	20 506
		α-Fe_2O_3	1 578	29 874			223	4 437		